UNIVERSITY OF COPENHAGEN

A thesis presented to the Faculty of Science in partial fulfillment of the requirements for the degree

Master of Science in Physics

Planet Earth-like patterns in three-dimensional multi-species bacterial colonies

Alba García Vázquez

mgx632@alumni.ku.dk

Supervisor: Liselotte Jauffred

August 2021

ACKNOWLEDGEMENTS

First and foremost, I would like to thank my supervisor Liselotte Jauffred for giving me the opportunity to work on this challenging but very fun project and for her enthusiastic guidance and support during this masters thesis. A special thanks to my fellow teammates Mireia Cordero Sánchez and Martin Møller Larsen for their invaluable company, collaboration, and good times in the laboratory. I would also like to give a special thanks to Miguel Garrido Zornoza for his support and for cooking croquetas after my long days in the lab. Last, but not least, I would also like to thank my friends and especially my family for their love, support, and their interest in this project.

ABSTRACT

Bacteria typically grow in communities and this provides them substantial advantages compared to solitary cells. These communities are often comprised of multiple bacterial species leading to the emergence of complex spatial patterns. The emergence of these complex spatial patterns can have a profound effect on bacterial function and survival within the communities. Most experimental studies investigating the mechanism behind this pattern formation have focused in two-dimensional systems. Here we propose a novel approach to study three-dimensional multi-species bacterial colonies. This three-dimensional setting replicates better some environmental bacterial habitats such as soil and intestines. Our method, consists overall in the encapsulation of bacterial cells of different species inside agarose beads and submerging them in soft agar. Later these growing colonies are imaged with advanced microscopy techniques. Here we show these colonies emerging from agarose beads have a window where they grow linearly and have a resulting planet Earth-like pattern. Our results indicate that in three-dimensional multi-species colonies just the cells from the outer part of the colony are able to grow while the center of the colony remains static. We anticipate our protocol to be a starting point for further studies. For example, the protocol could be used to bring some light to many different biological and physical questions which are still unanswered such as the mechanism behind horizontal gene transfer and the social interactions arising within multi-species three-dimensional bacterial colonies. Furthermore, understanding how bacteria thrive in competitive habitats and their cooperative strategies for surviving extreme stress can be instructive, for instance, to inspire new investigations for developing a more rational approach for battling pathogenic bacteria resistant to antibiotics.

CONTENTS

LIST OF FIGURES

LIST OF ABBREVIATIONS

GFP Green Fluorescence protein
RFP Red Fluorescence protein
LB Lysogenic broth
MM Minimal media
OD600 Optical density of a sample measured at a wavelength of 600 nm

Part I

INTRODUCTION

1

MOTIVATION

Bacteria are prokaryotic microorganisms with a typical length of $\sim 1\ \mu$m and usually rod or sphere shaped. In nature, bacteria rarely live by themselves as single-celled organisms but instead they grow in communities, whose structures are shaped by chemical, biological, and physical factors (Stoodley et al. 2002; Flemming et al. 2016; Stubbendieck et al. 2016). Cells within these communities or colonies have substantial advantages compared to solitary cells, such as increased resilience against external threats (Nadell, Drescher, et al. 2016). Microbial communities can be found in almost every habitat on Earth and affect many aspects of our lives. They can be devastating as infection and industrial contamination agents, but highly beneficial in their contribution to healthy microbiota, bioremediation, and biogeochemical cycles (Nadell, Foster, et al. 2010).

Colonies are often comprised of multiple bacterial strains and species, and these feature a diverse repertoire of social interactions such as competition (Hibbing et al. 2010) and cooperation (Ben-Jacob et al. 2000; Griffin et al. 2004). These interactions may lead to the emergence of complex spatial structures, which can have a profound effect on bacteria function and survival, and promote biodiversity, by optimizing the division of labor within the communities (Nadell, Drescher, et al. 2016). Spatial structure can also enhance horizontal gene transfer among different species (Cooper et al. 2017).

We are only beginning to understand how and why different genotypes arrange themselves in space as cells grow and divide (Nadell, Drescher, et al. 2016). The emergence of these patterns is usually

driven by nutrient limitation and stochasticity. Even when different strains or species are initially well-mixed populations sectors with low genetic diversity form within the colony, even among cells of similar fitness. This self-organization of microbial cell communities is the result of a genetic drift in a complex interplay with evolution, competition, and cooperation (Hallatschek et al. 2007).

The emergent spatial patterns generated by growing bacterial colonies have been the focus of intense study in physics during the last thirty years (Bonachela et al. 2011). So far, the vast majority of experimental studies that shed light on the mechanism behind this intricate pattern formation are done in two dimensions by inoculation of bacteria on agar structures (Hallatschek et al. 2007; Xiong et al. 2020). However, in nature, bacteria are often found in physically structured, spatially heterogeneous habitats, where at a minimum, cells vary in their access to nutrients depending on their position within the colony and thereby divide at different rates (Shao et al. 2017).

The aim of this thesis is to develop a protocol for growing multi-species bacterial colonies inside a solid medium such that a three-dimensional colony can form. This three-dimensional setting replicates better what happens, for instance, in some bacterial habitats such as soil and intestines. To develop the protocol we used two *Escherichia coli* bacterial strains tagged with two different color fluorescence proteins. Once the protocol was established, we investigated the growth dynamics of these colonies emerging from agarose beads and the intricate patterning they present imaging them with a confocal microscope.

2

THESIS OUTLINE

This thesis is divided into five parts. We start with Part ii, where we cover the main theoretical background of this work. This is followed with Part iii, where we explain step by step the protocol developed in this thesis to grow three-dimensional multi-species colonies. In Part iv, we show the results obtained in this work. These results are discussed in Part v. We conclude with Part vi, where we describe the conclusions and future work.

Part II

BACKGROUND

3

BACKGROUND

This chapter starts with an overview of the biological system to be studied. In section 3.1.1, the definition of bacterial growth is introduced along with the different phases in which bacteria grow in a spatially homogeneous environment. We then present a simple equation that can be used to describe the growth dynamics of a bacterial population in well-mixed liquid cultures, a condition in which bacteria are grown in the laboratory. However, as we discuss in section 3.1.2, in nature bacteria are found in spatially structured environments (Allen and Waclaw 2018). These spatially structured populations can be modeled with the so-called Eden Growth model. Within these structured populations, bacteria often experience multiple social interactions such as cooperation (Hibbing et al. 2010) and cooperation (Ben-Jacob et al. 2000; Griffin et al. 2004). That can lead to the emergence of complex spatial patterns. In section 3.1.3 we present the bacterium used in this project. Finally, We end this chapter, section 3.2, with a brief presentation of the tool used for the three-dimensional imaging of the bacterial colonies.

3.1 BIOLOGICAL SYSTEM: BACTERIA

Bacteria are procaryotic single-cells microorganisms that come in different shapes such as rods, spheres, or spirals, and have a typical size of a few micrometers in length. Therefore, they can only be seen under the microscope. Bacteria were among the first life forms to appear on Earth and are

present in most of its habitats, from water and soil to human or animal gut. Bacterial rarely live by themselves as single-celled organisms but instead, they grow in communities.

3.1.1 *Bacterial growth in a spatially homogeneous environment*

Bacterial growth consists of the conversion of chemical nutrients into biomass. Nutrients enter each bacterium through pores in its membrane and undergo a series of chemical transformations, at the end of which new cellular components are made. This increase in biomass is accompanied by the increase in cell size and by replication of the bacterial DNA, possibly with some errors (mutations). Eventually, the cell divides into two daughter cells, in a process called binary fission (Allen and Waclaw 2018).

The dynamics of growth of bacterial populations has been extensively studied for cells in well-agitated liquid cultures, where all cells have equal access to nutrients (Shao et al. 2017). In a liquid culture, bacteria experience four different growth phases (Humagain 2018). These different phases are shown in Figure 1. The initial phase is the *lag phase* where the growth is essentially zero because the bacteria need to adjust to the liquid medium (more precisely, to synthesise the necessary proteins to undergo cell division). This phase is followed by a phase of exponential growth, known as the *exponential phase*. Once growing cells have consumed the nutrient in the growth media or build up waste products during the exponential phase, they gradually transition to the *stationary phase* and eventually stop net growth. In this third phase cells still grow and divide but the number of new cells is balanced with the number of cells dying. The final phase of bacterial growth is the *death phase*, characterized by a net loss of viable cells, this is, cells in the colony die at larger rates than they are growing due to a depletion of resources, accumulation of toxic products, or external stresses killing the bacteria. Bacterial colonies in nature do not necessarily follow the previously mentioned phases. For instance, bacteria growing in colonies may compete for local resources, giving raise to non-trivial growth and the formation of complex patterns.

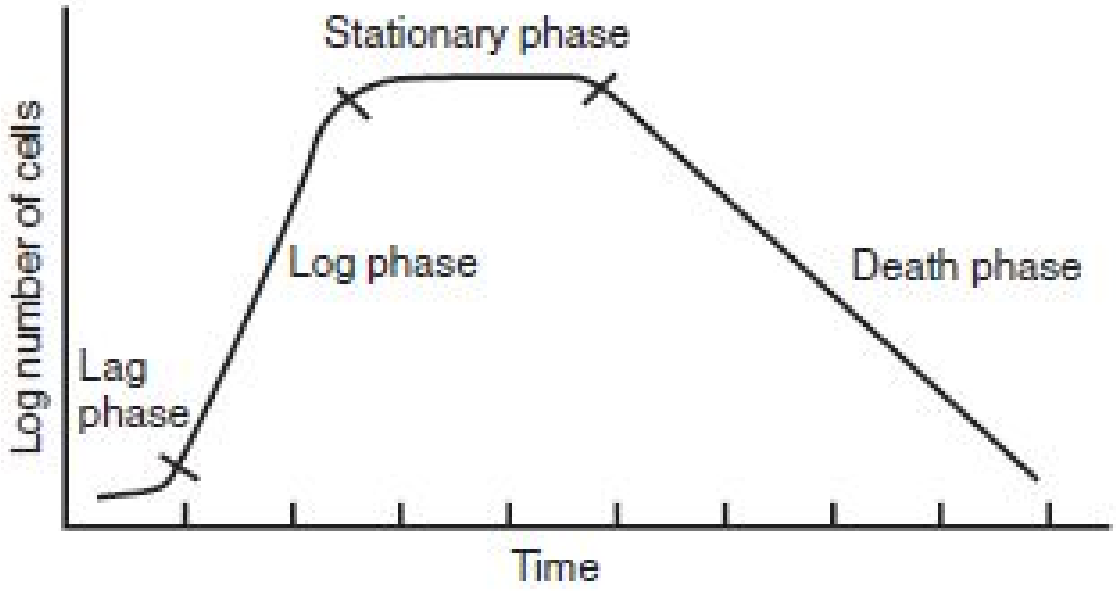

Figure 1: Bacterial growth curve in a well-mixed cell culture. The four different phases (*lag phase*, *log phase* or *exponential phase*, *stationary phase*, and *death phase*) can be differentiated by looking at the evolution of the number of cells in the culture, on a a logarithmic scale, over time. The first phase is known as lag phase, where the growth is essentially zero, and it corresponds to the time it takes the bacteria to adapt to the liquid medium (more precisely, to synthesis the necessary proteins to undergo cell division). Following the lag phase bacteria experience a phase of exponential growth, hence the received name of exponential phase. Once growing cells have consumed most nutrients in the growth media or built up waste products during the exponential phase, they gradually transition to the stationary phase and eventually stop net growth. Consequently, the death and growth rates are equal and the population number remains unchanged. The final phase of bacterial growth is the death phase, characterized by a net loss of viable cells. Cells in the colony die at larger rates than they are growing due to a depletion of resources, accumulation of toxic products, or external stresses killing the bacteria. Reprinted from (Humagain 2018).

Simple equations can be used to describe the dynamics of growth of bacterial populations in well-agitated liquid cultures (Allen and Waclaw 2018). Assuming initially that the nutrients are unlimited, the dynamics of the bacterial population can be described as

$$\frac{dN(t)}{dt} = rN(t), \tag{1}$$

where $N(t)$ is the number of bacteria at time t and r is the per-bacterium replication rate. Equation 1 predicts that the population grows exponentially, i.e.,

$$N(t) = N(0)\exp(rt). \tag{2}$$

Equation 1 is appropriate for relatively large populations ($\gg 10^3$ cells), and provides a good model for the exponential phase of growth of a bacterial population. However, it does not capture the transition to the stationary phase, where the population saturates. A simple way to capture this saturation is to use a logistic growth equation, a common S-shaped curve, where it is considered there is a maximum population size (Allen and Waclaw 2018).

3.1.2 *Spatially structured bacterial populations*

In nature, bacterial populations rarely exist as well-mixed, homogeneous, liquid cultures as mentioned in section 3.1.1. Instead, imperfect mixing, combined with spatial heterogeneity of the environment (e.g. gradients of food, oxygen, waste accumulation, temperature) leads to the emergence of populations that are spatially structured. These structured populations often take the form of dense colonies in which individual cells have different access to nutrients depending on their position. Furthermore, within the colony bacterial cells interact mechanically with each other, pushing against each other due to growth (Allen and Waclaw 2018). These mechanical forces play an important role in shaping the structure of the bacterial community (Xiong et al. 2020). However, the dynamics of bacterial growth

in such conditions is poorly understood (Shao et al. 2017).

The morphology of bacterial colonies can provide plenty of information about how the cells adapt and overcome different changes in the environment (Sousa et al. 2013). Møller Larsen 2021 and Cordero Sánchez 2021 in their master thesis develop a protocol for growing bacteria inside a solid medium such that a three-dimensional colony can form. These colonies arise when individual bacterial cells are submerged in soft growth media, pour into a plate, and allowed to proliferate in an incubator for $\sim$15 h. These colonies are visible by the eye as small spots of size $\sim$0.2 mm. Each one contains $\sim 10^6$ cells, all of which are the progeny of a single founder cell. Møller Larsen 2021 and Cordero Sánchez 2021 work with multiple bacterial strains whose main difference is the bacterial shape and the deletion of structures responsible for adhesion and motility processes. They observe a higher elongation in colony shapes as the stiffness of the media is increased and conclude that small fluctuations in the colony environment have a much larger impact on the colony morphology than that caused to the shape of individual bacterium or the deleted structures in the strains. More generally, the shape and size of a bacterial colony depends on factors such as the agar gel stiffness and the nutrient concentration (Allen and Waclaw 2018).

3.1.2.1 *Modelling spatially structured bacterial populations: Eden Model*

Many different approaches can be used to model spatially structured bacterial populations, depending on the system being studied and the desired level of physical and biological detail. In this section, we discuss an individual-based model known as the Eden model (Eden et al. 1961), where the position and state of each bacterial cell is tracked in time. The simplest form of an individual-based model of a bacterial population is a lattice-based one, in which bacteria occupy sites on a lattice and reproduce into neighboring lattice sites according to certain rules.

In 1961, Eden introduced a discrete stochastic growth model for tumor growth, which has become a standard model for describing the propagation of rough surfaces, such as bacterial colonies (Kuennen

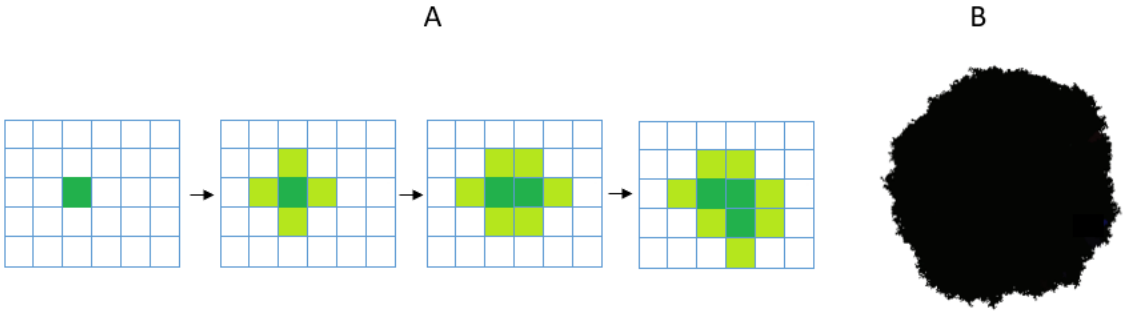

Figure 2: (A) Implementation in a two-dimensional square lattice of the Eden Model. The dark green squares represent occupied sites and the light green squares represent the available growth positions. The black arrows indicate the following time step. The model starts with a seed particle in the center of the lattice. In the second time step the available growth sites are found and one of them is chosen randomly and selected as a growth position. In the following time step, the lattice presents now two occupied sites, the now available neighbours are found and one of them is again chosen randomly as a growth position. The process can continue as many times as wanted. (B) A snapshot of a simulation of the 2D Eden model in which a cluster of cells (N = 65536) has grown from a single initial cell. Reprinted from (Allen and Waclaw 2018).

and C. Wang 2008). Figure 2A shows a diagram of the implementation of the Eden Model. In this lattice model, starting with a seed particle at the origin, at each iteration a new cell is added at random to one of the empty neighboring positions. As a result, this model is able to represent two and three dimensions radial bacterial colonies with irregular borders. Figure 2B the resulting cluster of occupied lattice sites produced by the Eden model.

3.1.2.2 *Social interactions within bacterial colonies*

Unlike free microorganisms, the various microorganisms in the colonies have diverse communication, cooperation and competition interactions, and are thus inundated with multiple non-linear interactions. Generally, colony formation has three advantages for the individual cells: 1) Plumping up to resist the adverse environment (antibiotic or other environmental stresses) (Nadell, Drescher, et al. 2016);

2) Provide nutritional ingredients that are difficult to acquire individually (Stevens et al. 2012); 3) Getting new genetic information by means of gene flow (Cooper et al. 2017).

Competition and cooperation are two main types of interaction inside bacterial colonies, and can take place both between the same species and among different ones. Generally, it is considered that the competition between microorganisms is an adverse behavior to the recipient bacteria in the interaction, while cooperation is a favorable behavior to the recipient bacteria (Bramhachari 2019).

Competition is a common ecological behavior inside the colonies. It is caused by the limited supply of space, nutrients, oxygen, and light. In addition, besides competing for nutrition and space, bacteria can also compete by excreting antibiotics, surfactants, toxins to kill or inhibit the accompanying bacteria (Bramhachari 2019).

Among with competition, cooperation is also a common ecological behavior among the residents inside the colonies. The phenomenon of cooperation was first discovered by comparing single cultivation and mixed cultivation of single bacterium colonies. It was found that the colony quantity significantly increased after mixed cultivation, indicating a (positive) collective effect between them, since the metabolites from each may serve as public goods that can be used by the rest as suggested by (S. Wang et al. 2015).

It should be pointed out that competition and cooperation should co-exist in the colonies, but the roles are different according to the species and environment. When the bacteria in the colonies are from the same environment, the strains inside the colonies are likely to cooperate. However, if they come from different environments, they might compete. On the other hand, the species type and genetic relationship also affect. If the members inside the colony have the same genotype, then it will benefit cooperation; otherwise, competition will likely take place (Burmølle et al. 2014).

3.1.2.3 *Patterning formation*

In section 3.1.2 we discussed how bacteria are more likely to live in physically structured habitats as colonies. These microbial populations are often comprised of multiple bacterial species and strains. These feature a diverse repertoire of cooperation and competition interactions as mentioned above and may lead to the emergence of complex spatial structures.

Pattern formation has been traditionally studied in bacterial colonies inoculated on surfaces with a high nutrient level and intermediate agar concentration. Such friendly conditions yield colonies of simple compact patterns (Ben-Jacob et al. 2000). However, the resulting patterns are very different for different nutrient concentrations (which strongly influence cell growth rate) and different agar concentrations (which control cell mobility by altering the hardness of the substratum on which the colony is expanding). For instance, Xiong et al. 2020 investigated how a colony containing both motile and non-motile species develops on a solid surface. Their experiment showed that when a droplet of liquid containing both species was placed on agar, both species grew and spread rapidly as if the non-motile hitchhiked on the highly motile cells. As a result, non-motile cells accumulate at the expanding boundary of the colony making it unstable and leading the growing colony towards the development of complex flower-like shapes (Figure 3). Experimentally, the patterning dynamics for a three-dimensional setting, more resemblant to bacterial habitats such as soil and intestines, has still not been studied.

Figure 3: Flower like patterns in mixtures of *E.coli* and *A. baylyi*. The pattern after 3 days of growth on a 0.5 % agar surface. Modified from (Xiong et al. 2020).

A very interesting feature of the growth of bacterial colonies is the spatial distribution of the descendants of a particular founder cell within the population. Local populations of bacterial are often established by groups of progenitors that proliferate into larger clusters. Experiments with bacterial colonies on agar have revealed that expanding cell groups can segregate into sectors that are each dominated by a single genetic lineage (Nadell, Foster, et al. 2010). The emergence of this macroscopic spatial pattern can have a profound microscopic effect on bacteria growth and survival (Nadell, Drescher, et al. 2016). Figure 4A shows the time evolution of a simple experiment in which a two-dimensional bacterial colony is started from a droplet containing a 1:1 mixture of two non-motile strains of *E. coli* which are identical except that they produce different-colored fluorescent proteins. The area covered by the initial droplet appears yellow, indicating a mixture of red and green cells. In

the surrounding regions, the populations have expanded out from the initial droplet producing red and green sectors. This implies genetic segregation: the descendants of different cells within the founder population occupy different regions of space.

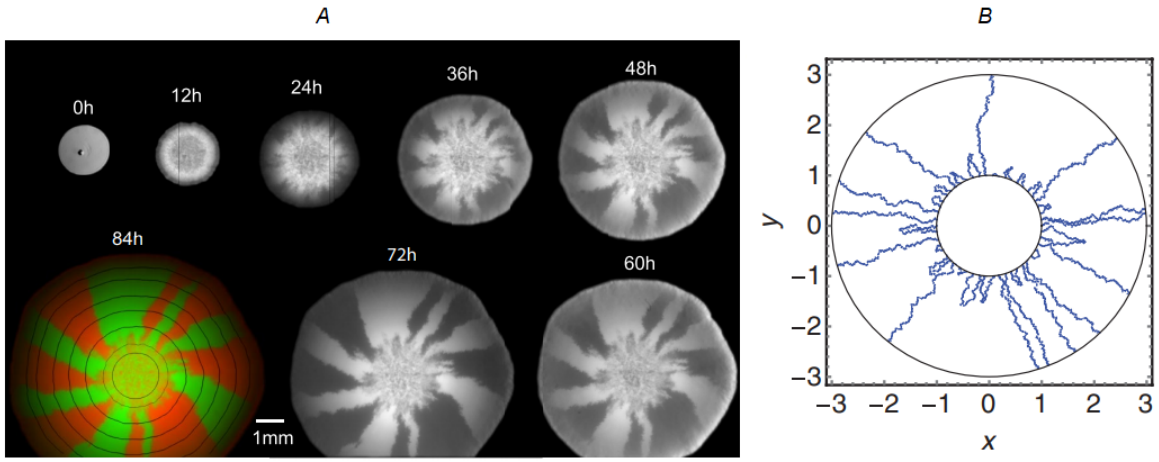

Figure 4: (A) Images, taken at 12-h intervals, of a growing colony founded by a 1:1 mixture of genetically identical bacterial strains ($\sim 10^6$ *E. coli* cells) except for expressing either cyan fluorescent protein (CFP) or yellow fluorescent protein (YFP). Even though the bacteria are otherwise genetically identical, the growing colony shows complete segregation of the two neutral markers (CFP and YFP) over time. The progression of the fluorescent images suggests that the dynamics of segregation is restricted to the edges of the colony, whereas, except for a gradual thickening, the interior distribution of CFP and YFP is essentially frozen. The bright-field image at 0 h indicates the initial extent of the founding population, which is mostly lined up on a circle (the central dark spot is a surface irregularity caused by the delivering pippete). Within 12 h and 72 h, the YGP signal is shown; at 84 h (final time point), YFP (green) and CFP (red) images are overlaid on each other with the physical boundary (black lines) of the growing colony at earlier times obtained from bright-light images. Modified from (Hallatschek et al. 2007). (B). Results of a simulation in which sector boundaries are modelled as annihilating random walks, as described by Equation 3 with $D = 0.02$, $R_0 = 1$, $R = 3$. The simulation starts with 50 random walkers. Reprinted (Allen and Waclaw 2018).

The emergence of these sectors is closely connected to the fact that, after an initial period of exponential growth, only bacteria that are close to the expanding edge of the colony are able to replicate; while the others are buried behind the front because deeper in the colony nutrient becomes

depleted and waste products may accumulate (Hallatschek et al. 2007). Demographic fluctuations at the growing colony front can cause a bacterial lineage to become trapped behind it, in which case it cannot proliferate further. Thus, a stochastic process is at play, in which some lineages come to dominate the growing front forming the sectors while the others are buried behind.

The arc length, w, occupied by a sector can be modelled by the following Langevin equation

$$\frac{dw}{dR} = \frac{w}{R} + \sqrt{4D}\nu(R), \tag{3}$$

with the initial condition $w(R_0) = w_0$, where R_0 is the initial radius of the circle (the radius of the drop of bacteria that is deposited on the agar). $R = vt$ is the radius of the circle where the proliferating bacteria are located expanding with constant velocity v. The growing layer is infinitely thin and circular symmetric. D is an effective diffusion constant, and $\nu(R)$ represents an uncorrelated Gaussian noise with zero mean and unit variance. In Equation 3, the first term on the right hand side accounts for the radial expansion of the colony, which stretches the sector. The second term accounts for stochasticity in the replication events and local movements of bacteria at the front.

One important parameter that affects the formation of sectors is the initial density of founder cells. Using *Bacillus subtilis* Van Gestel et al. 2014 shows both experimentally and by mathematical modelling, that colony growth can result in spatial segregation of lineages, and that the degree of heterogeneity is strongly related to the initial density of founder cells. At low initial cell densities co-cultured strains strongly differentiate in space, whereas spatial separation does not occur at high initial cell densities.

Figure 5 shows the effect of initial cell density on the spatial segregation of two co-cultured strains in a colony. At the onset of colony growth, founder cells are distributed randomly and separated from each other, where the degree of separation is highest at low initial densities. By means of cell division, the founder cells grow into small cell clusters that only start to merge upon contact. Getting into contact takes longer when the initial distance between founder cells is larger. Accordingly, colonies started by a small number of founders will be structured much more in the initial phase of colonies

growth than colony started with a high density of founders (Van Gestel et al. 2014). At later stages, the differences in spatial patterning might become smaller due to the dynamics of colony growth (Nadell, Drescher, et al. 2016).

3.1.3 *Escherichia coli*

Escherichia coli (*E. coli*) is the "workhorse" of the microbiology lab and it was the bacteria chosen for our project since it is very easy to grow under laboratory conditions, and very safe to work with. *E. coli* is the most well-understood bacterium in the world. It is known it is a rod-shaped bacterium whose cells are approximately 0.8-1 μm in diameter and approximately 2-4 μm in length (Allen and Waclaw 2018). It can divide every 20 min in the laboratory under aerobic, nutrient-rich conditions, which allows many generations to be studied in a short time. *E. coli* is a normal inhabitant of the human gastrointestinal tract and may occasionally be associated with diseases in humans. Physiologically, *E. coli* is versatile and well-adapted to its characteristics habitats (e.g. the bacterium can grow both in the presence or absence of O_2).

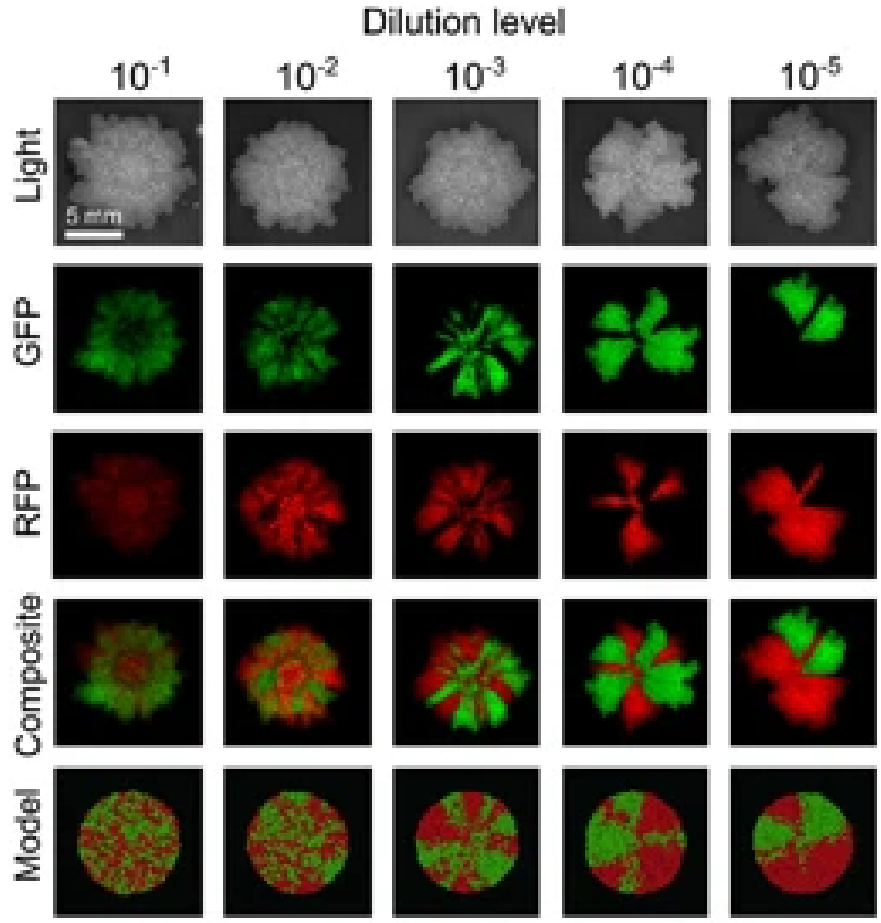

Figure 5: Effect of initial cell density on the spatial segregation of two co-cultured strains. From top to bottom: bright field images, green-fluorescence images (GFP), red-fluorescence images (RFP), composite images, and simulation results. Inoculation of two different strains, each tagged with either red or green markers, but otherwise genetically identical, at various initial cell densities: 10^{-1}, 10^{-2}, 10^{-3}, 10^{-4}, 10^{-5} cells/ml. The dilution levels only apply to the biofilm images and not to the simulation results. For the simulation results, ten replicate simulations were initiated with 10, 20, 50, 100, or 200 founder cells, respectively. Half of the cells (and their descendants) were marked red and the other half were marked green. The scale bar is equal to 5 mm. Reprinted from (Van Gestel et al. 2014).

3.2 IMAGING THREE-DIMENSIONAL COLONIES

Over the past several centuries, humans learned to manipulate light to peer into previously invisible worlds (Parker et al. 2018). By using various techniques to manipulate color, size, and contrast the microscope has opened views within the microcosm of the natural world (Pelc et al. 2020).

To select the right microscope, the key question we have to ask ourselves is what is the biological question we want to answer and what must one measure to answer it (Jonkman et al. 2020). In this thesis, the goal is to investigate the spatial arrangement of fluorescent molecules so this leads us to choose a Confocal Microscope since it is an excellent tool for making quantitative measurements in cells with high contrast images of fluorescent light sources and also allows to perform optical sectioning.

3.2.1 *Fluorescence Imaging*

Fluorescence microscopy is based on fluorescent probes that target specific molecules or cells. Fluorescence is the emission of light that occurs within nanoseconds after a fluorescent molecule absorbs light of a certain excitation wavelength that is typically shorter. When a fluorophore absorbs light, all the energy possessed by a photon is transferred to the an electron from the ground state and it is excited to a higher unoccupied molecular orbital. The time it takes the electron to transition from the ground state to an excited state is extremely brief. Once excited, the electron uses several two-step pathways to lose the absorbed energy and return to the ground state. First, the electron relaxes by a non-radioative process to one of the lower vibrational sublevels. Then, the electron relaxes back to the ground state by emitting a photon. Because the emission starts from the lowest vibrational level, the energy of the emitted photon is typically less than the absorbed photon (Lichtman and Conchello 2005). The difference between the exciting and emitted wavelengths, is known as the *Stokes shift*.

Figure 6 shows the two spectra of a fluorescent molecule: the excitation spectra gives the probability that a molecule will be excited by light of a specific wavelength and the emission spectra gives the probability a molecule will emit a photon of a certain wavelength. By completely filtering out the exciting light without blocking the emitted fluorescence, it is possible to see only the objects that are fluorescence (Lichtman and Conchello 2005). A common problem of fluorescence microscopy is photobleaching, an alteration of a fluorophore molecule such that it can no longer be detected because it is unable to fluoresce permanently. It can happen due to long exposure of a sample or exposition to a very high intensity light.

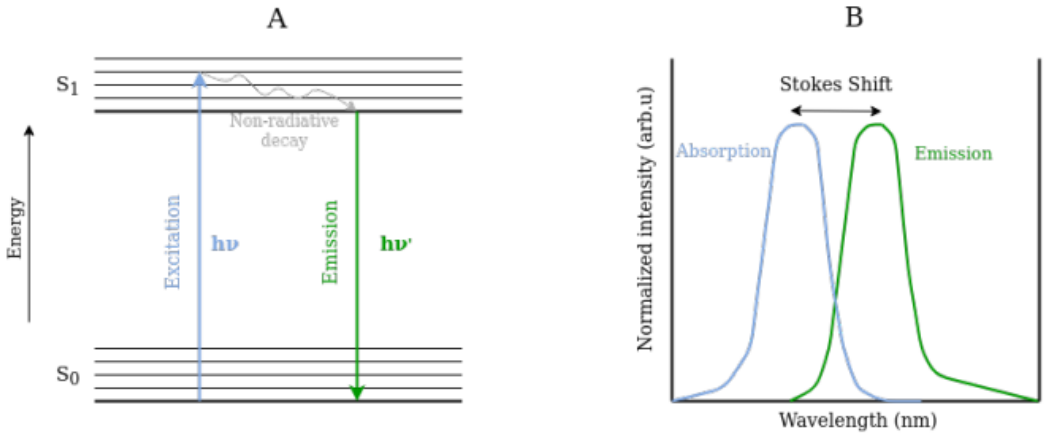

Figure 6: Concept of fluorescence. (A) Light excites an electron from the ground state S_0 to a higher vibrational or excited state S_1. The electron first relaxes to a lower vibrational sublevel of S_1 by a non-radioative decay, and then relaxes to the ground state emitting fluorescence light in the process. (B) Example of excitation and emission spectra for a fluorophore. Reprinted from (Cordero Sánchez 2021).

3.2.2 *Confocal Microscopy: Imaging in three dimensions*

Confocal microscopy is an excellent tool for making measurements in cells and fluorescence quantification with high spatial precision (Jonkman et al. 2020). Confocal microscopes aim to overcome resolution limitations of traditional wide-field fluorescence microscopes(Jonkman et al. 2020).

Figure 7 shows a schematic of the main components and the lightpath in a Confocal Microscope. In a Confocal Microscope a laser beam acts as the excitation source. This laser beam is reflected by a dichromatic mirror (beam splitter) and focused into a specimen, where it excites its fluorescent molecules throughout the entire cone of illumination. The light emitted by these excited fluorescent molecules is collected by the objective lens and focused by a second lens (pinhole lens) through a carefully aligned pinhole. The pinhole ensures that only fluorescence that originates at the focal point is captured by the detector, i.e, fluorescence emission from above or below the focal plane is blocked. The fluorescence is then detected. By successively scanning multiple Z-planes (or slices) the Confocal Microscope produces numerous two-dimensional, high-resolution images at various depths (or Z-stacks), which can be constructed into a three-dimensional image by a computer. This enables the reconstruction and quantification of the half sample volume (Jonkman et al. 2020).

To generate optical sections the confocal microscope has to be accompanied with a high-resolution objective lens (Jonkman et al. 2020). The most significant factor in determining both sensitivity and resolution is the numerical aperture, NA, of the objective (Jonkman et al. 2020). A higher numerical aperture increases the resolution of the system but at the same time limits the depth at which the sample can be imaged. That it is because a bigger numerical aperture decreases the distance from the objective lens to the sample. The NA is defined by the product of the sinus of the half-angle of the cone of light that is focused or collected by the objective, θ, and the index of refraction of the mounting medium, n (Equation 4)

$$NA = n \cdot \sin\theta. \tag{4}$$

The resolution limits the smaller feature that the microscope is able to discriminate. The lateral (XY) resolution of a fluorescence microscope depends on the wavelength λ of light and on the NA of

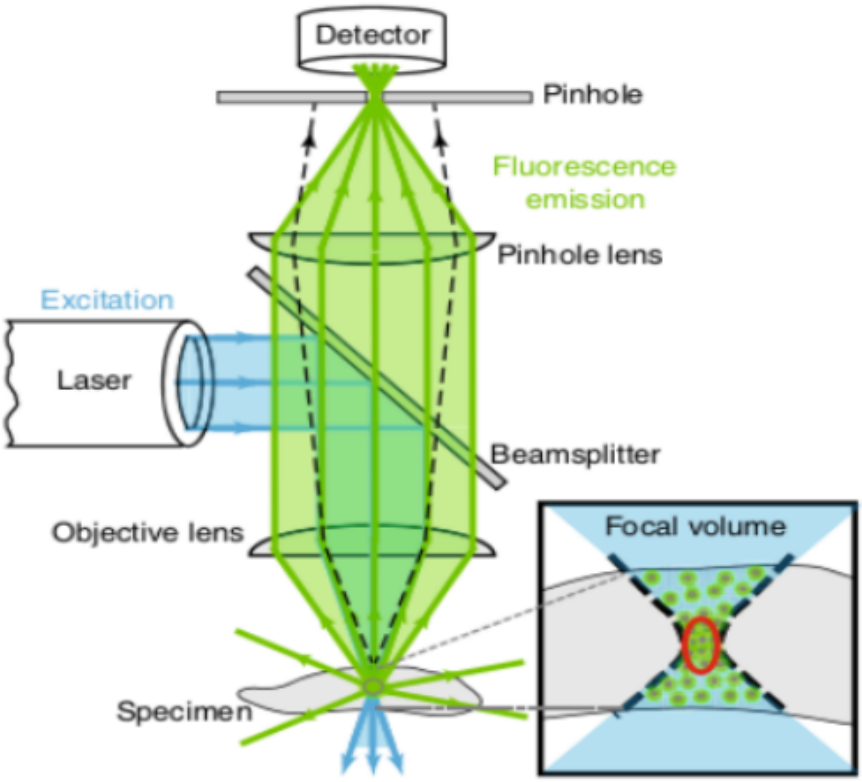

Figure 7: Scheme of a Confocal Microscope. In a Confocal Microscope a laser beam acts as the excitation source. This laser beam is reflected by a dichromatic mirror (beam splitter) and focused into a specimen, where it excites fluorescent molecules throughout the entire cone of illumination. The light emitted by these excited fluorescent molecules in the focus (red oval) is collected by the objective lens and focused by a second lens (pinhole lens) through a carefully aligned pinhole. The pinhole ensures that only fluorescence that originates at the focal point is captured by the detector. Light emitted by fluorescent molecules located outside the focus is not focused through the pinhole and therefore does not reach the detector (black dashed lines). The light is then detected with a detector. Reprinted from Jonkman et al. 2020.

the objective lens. Rayleigh's criterion is a rule of thumb for estimating the smallest features that can be resolved laterally (Equation 5)

$$R_{xy} = \frac{1.22\lambda}{2NA}. \tag{5}$$

Another important factor is the penetration depth. It estimates how deep light or any electromagnetic radiation can penetrate into a material. For Confocal Microscopes, due to absortion and scattering events, the penetration depth is generally limited to 50-100 μm.

Part III

METHODOLOGY

4

MATERIALS AND METHODS

In the starting section, 4.1, the baseline strain used as proof of method to develop a protocol for growing multi-species colonies in three dimensions is presented. In section 4.2, the novel protocol for growing multi-species colonies in three dimensions is established and explained step by step. Finally, in section 4.7, the image processing workflow followed in this project is described.

4.1 BACTERIAL STRAINS

In this thesis, we used two identical *E. coli* strains, labelled with two different fluorescence colors from Smith et al. 2017 as basis of a protocol for growing three-dimensional multi-species colonies inside a solid medium. Our *E. coli* strain *(REL606)* has been used in the laboratory for many decades for the ease of being cultured and stored under a variety of conditions. This strain carries no plasmids and harbors no functional bacteriophages; it is strictly asexual (Lenski et al. 1991). It can produce colonies on minimal medium but is unable to grow on the sugar *L-arabinose (Ara$^-$)* (Lenski et al. 1991). It is resistant to coliphage *T6* but sensitive to other T-phages, included *T5* (Lenski et al. 1991). It is characterized for being a thin and long bacteria with a width of (0.73 ± 0.04) μm, a length of (3.04 ± 0.57) μm and a volume equal to (1.19 ± 0.36) μm^3 (Monds et al. 2014). To this strain Smith et al. 2017 separately introduced either pmaxGFP (Lonza 2002) or pTurboRFP (*Evrogen*) plasmids for confocal microscopy (see Appendix 9 for more detail about the plasmids). The resulting *E. coli*

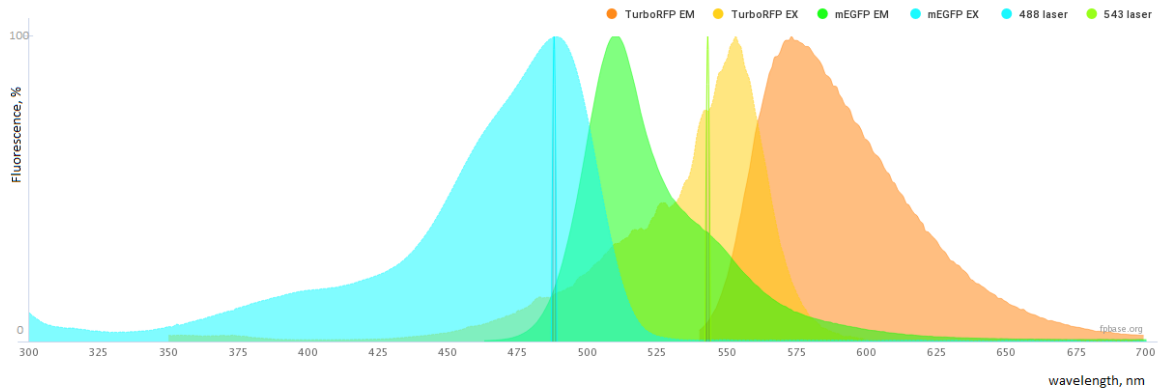

Figure 8: Plasmid Spectra of the red fluorescence protein used in this project (TurboRFP) and a green fluorescence protein (mEGFP) that has similar features to the green fluorescence protein used in this project, pmaxGFP (FPbase 2021). The excitation spectra for the green fluorescence protein (mEGFP) and the red fluorescence protein (TurboRFP) has a maximum of 488 and 553 nm, respectively. The emission spectra for mEGFP and TurboRFP has a maximum of 510 and 574 nm. The green and red fluorescence proteins can be excited with a laser of wavelength 488 nm (blue vertical line) and 543 nm (green vertical line) ,respectively, that is available in our confocal microscope setup.

strains are genetically identical except they carry different fluorescence proteins, either green or red. They are characterized by a max excitation/ max emission of 487 nm/509 nm and 553 nm/574 nm for the Green Fluorescent Protein and the Red Fluorescent Protein, respectively. Figure 8 shows the spectra of the fluorophores pTurboRFP and GFP similar to pmaxGFP.

4.2 PROTOCOL FOR GROWING THREE-DIMENSIONAL MULTI-SPECIES COLONIES

The novel protocol for growing three-dimensional multi-species colonies I developed is based on the methods by Buffi et al. 2011, where they develop and test a miniaturized bacterial biosensor. In their paper, the signal element in the biosensor is a nonpathogenic laboratory strain of *E. coli*, which produces a variant of the green fluorescent protein after contact with arsenite and arsenate. The *E. coli* bioreporter cells were encapsulated in agarose beads and incorporated into a microfluidic device

where they were captured in microcages and exposed to aqueous samples containing arsenic. The resultant green fluorescence signal is proportional to the arsenite concentration on the sample.

In this section, the protocol is established and it is explained step by step. Overall it consists of: encapsulating different bacterial species inside agarose beads, size-fraction these beads between 40 and 70 μm, and freeze the beads by mixing them with glycerol. The frozen beads are then stored at -80°C. Three-dimensional colonies can grow by submerging these beads inside soft agar and pouring their content in a glass-bottomed Petri dish. Figure 9 shows a comparison of the method I developed to grow multi-species three-dimensional bacterial colonies and the methods that have been usually followed to study multi-species colonies. The protocol is illustrated in Figure 10 and Figure 11 and reads as:

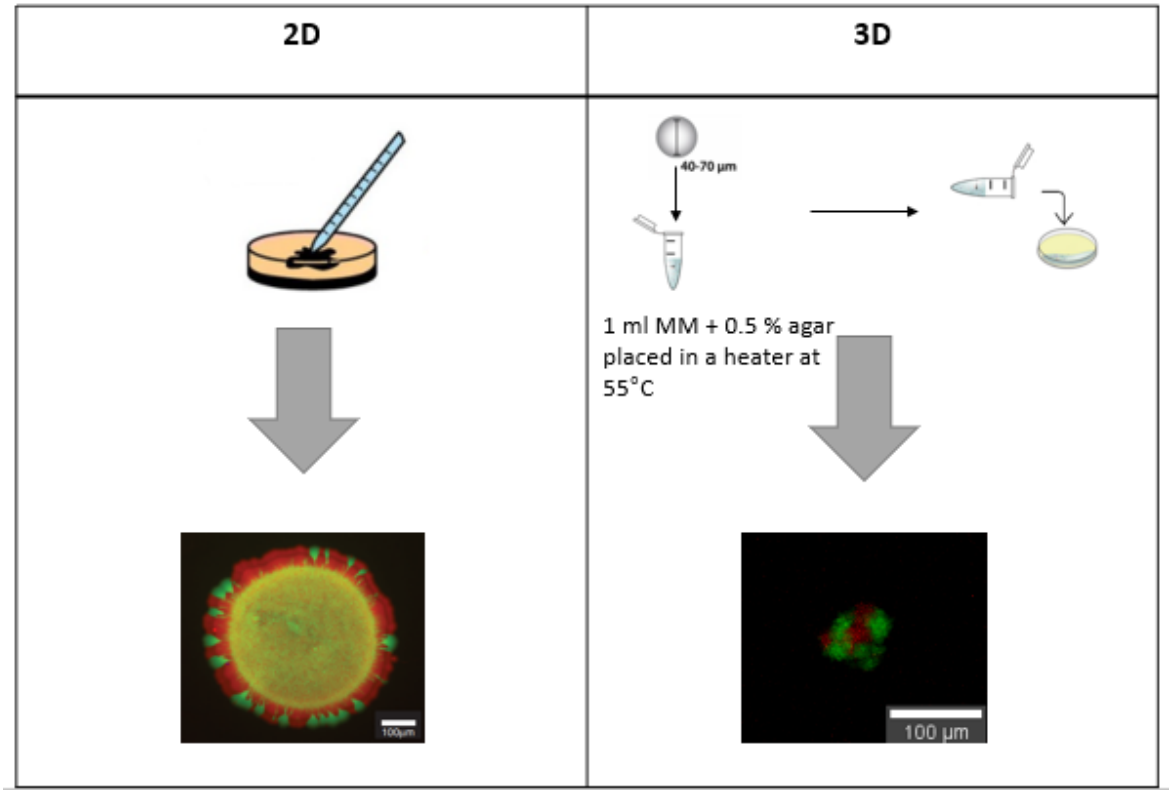

Figure 9: Comparison of the protocol followed to grow two-dimensional (2D) vs three-dimensional (3D) multi-species colonies. On one hand, two-dimensional experiments are carried by inoculating a droplet (yellow) containing a mix of bacteria on hard agar surfaces. When the mixed bacteria have the same fitness and are non-motile the populations expand out from the initial droplet producing sectors (red and green). On the other hand, three-dimensional colonies can grow by submerging agarose beads containing mixed bacteria inside soft agar and pouring its content in a glass-bottomed Petri dish.

Materials

- Milli-Q water
- *VWR Life Science* Agarose
- Pluronic F-68 solution 10 % Sigma
- Falcon tube
- Silicone oil (dime-thylpolysiloxane, Sigma)

- Ice
- Phosphate buffered saline solution (*PBS*)
- Glass pipette tubes
- 50 % glycerol
- LB media (see Appendix 10)

Equipment

- AccuBlock Digital Dry Baths, Labnet International, Inc.
- Thermomixer comfort Eppendorf 2 ml
- Microwave
- Vortex Mixer, Labnet International, Inc.
- Centrifuge 5804 R, Eppendorf
- Cell strainer 70 μm Nylon, BD Falcon
- Cell strainer 40 μm Nylon, BD Falcon

1) Encapsulation of multi-species bacterial cells in agarose beads

Step 1

Starting from a single colony, grow the red and green cells separately in 2 ml of *LB* medium supplemented with 30 μg/ml kanamycin at 37 °C for $\sim$8 h under constant shaking (150 rpm) (see Appendix 11). The final concentration of cells in both overnight cultures should be of the order of $\sim 10^9$ cells per ml.

Step 2

Preheat the material needed for the bacterial cell encapsulation in the agarose beads:

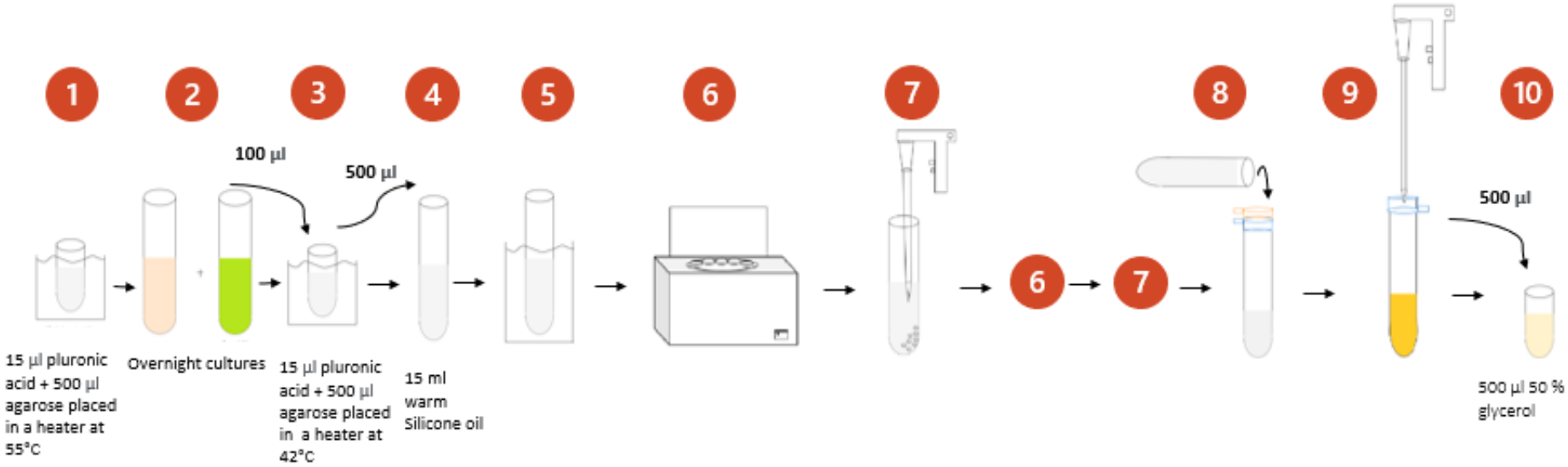

Figure 10: Encapsulation of multi-species bacterial cells in agarose beads. 500 μl of 2.5 % (w/v) agarose solution and 15 μl of pluronic acid is added to a 2 ml Eppendorf tube placed in a heater at 55 °C (1). The encapsulation procedure is continued at 42 °C and 100 μl of the mixed of red and green grown cell cultures (2) is added to the agarose-pluronic acid mixture with continuous mixing at high speed vortexing (3). The cell-agarose-pluronic acid mixture (500 μl) is added drop by drop with warm pipette tips into warm 15 ml of silicone oil (4). After 2 more minutes of continuous vortexing, the tube containing the cell-agarose-silicon mixture is plunged into a water-ice bath for 10 min (5). Beads are harvested by centrifugation for 10 minutes at 550 · g at room temperature (6). Afterwards, the oil is carefully removed first by pipetting, and then by rinsing with 5 ml of PBS solution (7) follow by bead centrifugation, pipetting oil from the surface, and then by rinsing again with 5 ml of PBS. Beads are size-fractionated between 40 and 70 μm, by collecting the flow-through from a 70 μm strainer and a 40 μm strainer (8). To make sure that the vast majority of the beads smaller than 70 μm and bigger than 40 μm go through the strainers 5 ml of PBS are poured through them as an additional washing step. Beads retained on the 40 μm filter surface are recovered by rinsing with 6 ml of LB solution (9). For the preparation of freezing cell-beads, 500 μl of the LB-bead solution are briefly mixed with 500 μl of 50 % glycerol-LB solution and then place and store at -80 ° C (10).

- Preheat the pipettes tips needed for the bacterial cell encapsulation by keeping them in an incubator set at 60 °C.
- Preheat 15 ml of silicone oil (contained in a 50 ml falcon tube) in a heat bath at 55 °C. Let it be there for ∼20 min until the temperature stabilizes.

Step 3

Place one 2 ml Eppendorf tube in a block heater at 55 °C. To ensure an uniform heating of the sample fill the holes with demineralized water.

Step 4

Heat a sterile mix of 2.5 % agarose solution[1] and Milli-Q water in the microwave until the agarose is completely melted. Let it cool down until is at ∼55 °C

Step 5

In the 2 ml Eppendorf tube set in the block heater at 55°C add the following components in sequence and let it rest until the temperature stabilizes (see Figure 10, step 1).

1. 500 μl of the cooled down agarose solution
2. 15 μl of pluronic acid

Step 6

Move the 2 ml Eppendorf tube containing the agarose-pluronic acid mixture to a thermomixer set at 42°C.

Step 7

Mix in the same falcon tube both green and red grown cell cultures (see Figure 10, step 2).

Step 8

Take 100 μl of the green-red cell mix and add it to the agarose-pluronic mixture at 42°C (see Figure 10, step 3).

1 Agarose is a polymer of agarobiose monomers, whereas agar is a natural product produced by algae that contains a mixture of agarose and agaropectin.

Step 9

Add very quickly drop by drop (with warm pipette tips so it does not solidify) 500 μl of the cell-agarose-pluronic acid mixture into the warm 15 ml of silicone oil (see Figure 10, step 4). It has to be added very quickly because it solidifies at temperatures below 25°C.

Step 10

Vortex at high speed the cell-agarose-pluronic acid-silicone oil mixture.

Step 11

Plung the cell-agarose-pluronic acid-silicone oil mixture in a water-ice bath for 10 min (see Figure 10, step 5).

Step 12

Harvest the beads by centrifugation for 10 min at 2000 rpm (500 $\cdot$ g, where g is the acceleration at a free fall in vacuo due to gravity) at room temperature (see Figure 10, step 6).

Step 13

Remove carefully the silicone oil by pipetting it (see Figure 10, step 7).

Step 14

Rinse with 5 ml of *PBS* solution.

Step 15

Centrifugate the beads for 10 min at 2000 rpm (500 $\cdot g$) at room temperature.

Step 16

Pipette carefully the silicone oil. Repeat the rinsing procedure once more with 5 ml of *PBS* solution.

Step 17

Size-fractionate the beads to arange between 70 and 40 μm in diameter by collecting the flow-through from a 70 μm strainer and a 40 μm strainer in a new sterile falcon tube (see Figure 10, step 8).

Step 18

As an additional washing step, pour through the 70 and 40 μm strainers 5 ml of PBS to make sure that the vast majority of the beads smaller than 70 μm and bigger than 40 μm went through.

Step 19

Put the 40 μm strainer upside down in a new sterile falcon tube and recover the retained beads on the filter surface by rinsing it with 6 ml of *LB*. The final bead concentration is $\sim 8 \cdot 10^3$ beads/ml (see Figure 10, step 9).

Step 20

For the preparation of freezing cell-beads, mix 500 μl of the LB-bead solution with 500 μl of 50 % glycerol-LB solution in a 2 ml Eppendorf tube and then place and store at -80°C (see Figure 10, step 10). For every experiment it is possible to make 12 stocks of cell-beads.

2) Embedment of agarose beads

Step 1

When the experiment wants to be carried out, take one of the cell-beads stock from the freezer and let it stay at room temperature for ∼5 min until melted.

Step 2

While the bead solution melts prepare the *M63* minimal media:

1. Place a 2 ml Eppendorf tube in a heat bath at 55 °C. To ensure an uniform heating of the sample fill the holes with demineralized water.

2. Warm in the microwave a bottle of 20 ml of 0.625 % agar + Milli-Q water until the agar is fully melted.

3. When the bottle is cold enough add: 5 ml of 5x*M63* salt, 25 μl of 1 mg/ml *B1* stock solution, 50 μl of 1M $MgSO_4$, and 250 μl of 20 % w/v *glucose*. Mix the solution. The resulting percentage of agar is now 0.5 %.

4. Quickly add 1 ml 0.5 % agar + *M63* minimal media solution to the 2 ml Eppendorf tube in the heat bath at 55 °C to keep the agar in a liquid state.

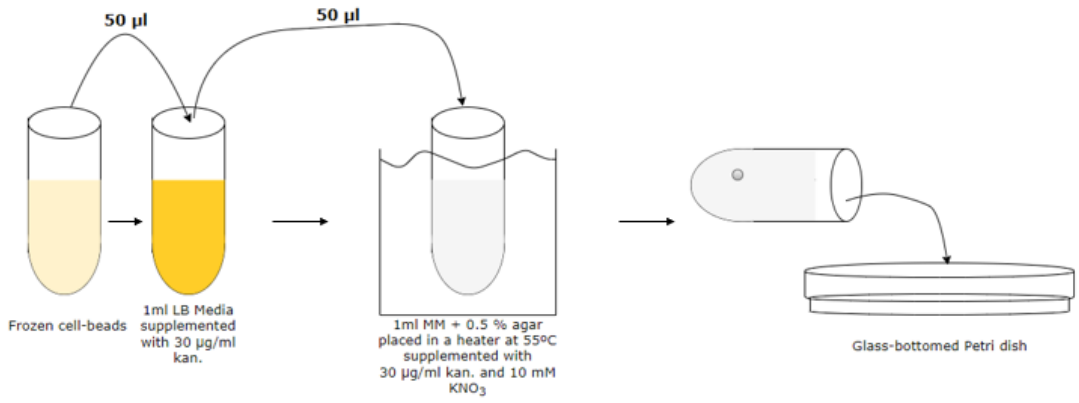

Figure 11: Embedment of agarose beads. The frozen cell-bead stocked is left at room temperature until melted. 50 μl from the melted bead-solution is diluted in 1 ml of LB supplemented with 30 μg/ml kanamycin (kan.). 50 μl of the dilution are added to a 2ml Eppendorf tube containing 1 ml M63 Minimal Media (MM) supplemented with 10 mM of KNO_3 and 30μg/ml of kanamycin at 55 $^\circ$ C. The mixed solution is poured into a small Petri dish and leave undisturbed on the bench for $\sim$5 min for solidification. After the inoculum dries on the plate, the plates are incubated at 37 $^\circ$ C for 5 h.

Step 3

When the bead solution is melted, take 50 μl and dilute it in 1 ml of LB media supplemented with 30 μg/ml kanamycin.

Step 4

Supplement the 1 ml 0.5 % agar + *M63* minimal media solution with 10 mM of KNO_3 and 30μg/ml of kanamycin and add 50 μl of the diluted bead solution. These dilution levels correspond to approximately 10-20 beads per ml.

Step 5

Quickly mix the content of the 2 ml Eppendorf tube and pour it into a glass bottomed Petri dish. Let the inoculum dry undisturbed for 5 min to let the agar solidify. The final thickness of the agar layer in the Petri dish is $\sim$ 300 μm. When the agar is solidified place it in the incubator and let the colonies grow for 5 h at 37°C.

4.3 IMAGE ACQUISITION: MICROSCOPY IMAGES

The colonies were imaged with a *LEICA SP5* confocal microscope (see Figure 12A) and a *NplanL20x0.40NA* objective. The 20 x objective was chosen to visualize the colonies, since objectives with higher magnification have smaller apertures and the red signal intensity emitted by the cells was very low to image them with greater precision.

One colony per experiment was imaged after being grown for 5 h in the incubator (the approximate time that takes the cells to reach the surface of the bead. This facilitates the task of finding them in the agar plate under the microscope). The Confocal Microscope was equipped with a heated stage set to 38 °C that allowed the colonies to grow while they were being imaged. The colonies were imaged every 15 min for 5 h. The Z-stack was taken sequentially, first with a red and then a green laser beam (488 and 543 nm respectively). Since the intensity level of the red fluorescence was very low, the colonies were imaged every time step first with the red laser and then with the green laser to minimize the bleaching of the red fluorophore. The detected wavelengths were: from 498 nm to 536 nm and from 568 to 641 nm for the green and red fluorescence, respectively.

All images were acquired under the same settings: a 20x air objective and a Z-step size equal to 1.33 μm and a number of steps equal to 151 [2].

With a 20x air objective (NA = 0.4), one can distinguish structures labelled with green fluorophores (λ ∼488 nm) with ∼744 nm lateral resolution. For structures labeled with red fluorophores (λ ∼ 543nm), the lateral resolution is equal to ∼828 nm. The depth resolution is about two to three times worse than lateral resolution ∼ 1860 nm and ∼2070 nm for green and red fluorophores, respectively (Equation 5).

The steps followed to image the colonies were the following:

2 On a confocal microscope, the software reports the slice thickness as the pinhole size is changed, and then automatically calculate the optimal Z-interval based on the Nyquist sampling theory of two to three overlapping z-steps per optical slice thickness.

1. Turn on the microscope and the heat stage and set it at 38 °C. Let the temperature stabilize for a minimum of 30 min.

2. Fix the heat stage to the stage of the microscope to minimize any kind of movement.

3. Once all the setup is properly mounted bring the Petri dish from the incubator and place it on the stage.

4. Find a bead and fix the plate to the stage with some tape to minimize the movement of the sample (see Figure 12B).

5. With the green laser find where the colony starts (when you start to see some fluorescence), subtract 50 μm and set it as the initial Z to start the Z-stack (Z-begin). To this Z-begin sum 200 μm and set it up as the final Z value where to stop the Z-stack (Z-end). This translates in a number of steps of 151 with a Z-step size of 1.33 μm.

6. Find the optimal gain value to see properly the green and red fluorescence.

7. Set to detect just wavelengths within 498-536 nm for the green fluorescence and within 568-641 nm for the red fluorescence.

8. Start the image acquisition: set the time-lapse for one image every 15 min, first the red and then the green laser for 5 h (the time-lapse settings should be saved in the microscope in order to repeat the experiments under the same settings).

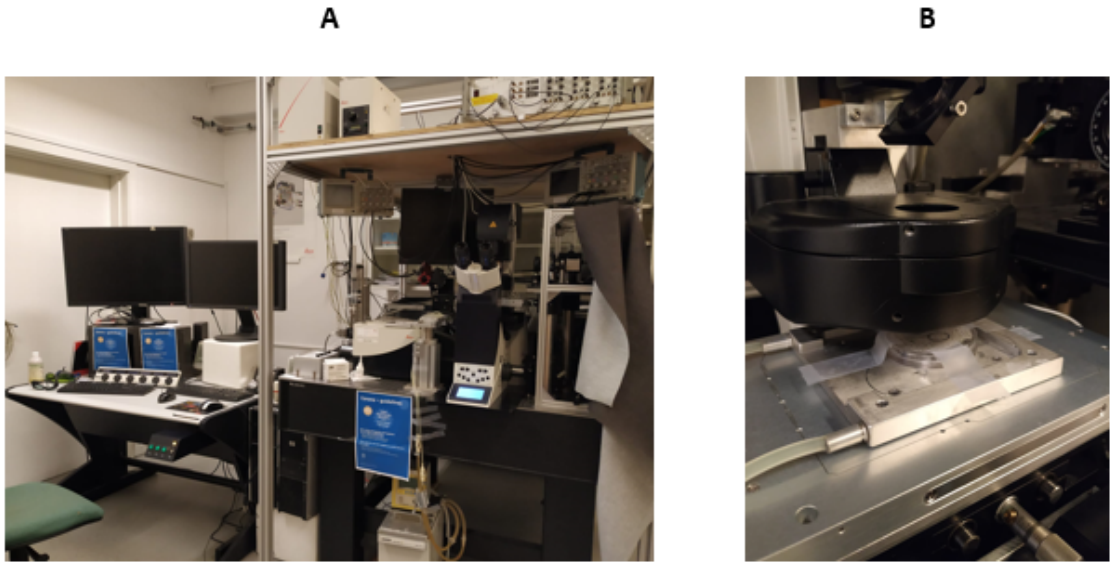

Figure 12: Microscope set up. (A) Confocal Microscope used in this thesis to image the colonies in three dimensions. (B) The heat stage is fixed to the stage of the microscope and the Petri dish Plate is fixed to the heat stage with some tape. The heating stage is connected to a heating system set to 38 °C.

4.4 COUNTING FORMED COLONIES

A colony-forming unit (CFU) is a unit used to estimate the number of viable bacteria in a sample. Viable cells are those with the ability to multiply via binary fission. The CFU assumes that every colony is separate and founded by a single viable microbial cell. Estimation of microbial numbers by CFU will, in most cases, undercount the number of living cells present in a sample since, for instance, the progenitor of the colony can be a mass of cells deposited together.

The experiments counting colony forming units were done by ten-fold diluting multiple times the overnight cultures of red and green cells (they are grown separately and mixed afterwards) on 1 ml of LB (or PBS, Pluronic Acid, or Silicone Oil for some experiments). 50 μl of the diluted overnight cultures are then plated in a Petri dish of LB + 1.5 % agar and spread with a sterile bacterial cell spreader and incubated overnight at 37 °C (see Figure 13 A). Figure 13B shows one example of a plate with a countable number of bacteria and definition of CFU.

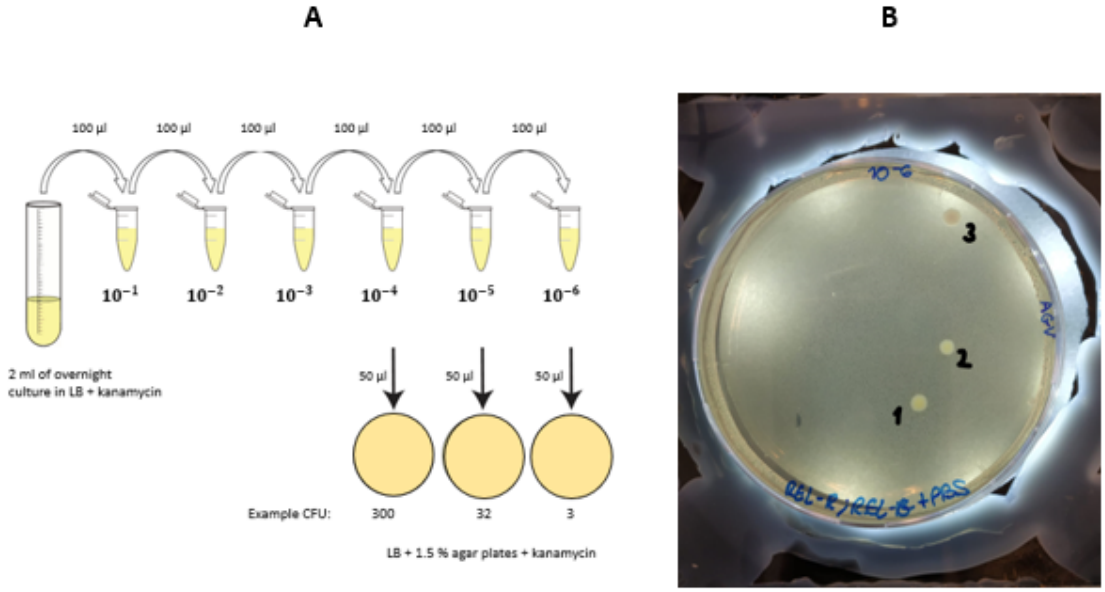

Figure 13: Counting colony forming units. (A) 2 ml of an grown overnight solution of red and green bacteria is serially diluted in 1 ml of LB (or Silicone Oil, PBS, or Pluronic acid) by taking 100 μl of the previous dilution levels. 50 μl of the dilutions are taken and plated in a Petri dish to count the number of viable bacteria. (B) The plate shows 3 colonies, or CFU. The dilution level of the plate is equal to 10^{-6}.

4.5 BEAD SHAPE AND SIZE DETERMINATION

To characterize the bead shape and size of the agarose beads the fresly made beads-LB solution where look under a microscope. The experiment was done by following the methods described in section 4.2. From the freshly bead-LB solution obtained, approximately $\sim$50 μl was introduced in precision cover glasses and looked under the microscope (*Nikon Eclipse Ti*) with a 20x/0.45 air objective (*SPLANFluor ELWD 20x/0.45 Nikon*).

4.6 FLUORESCENCE LEVEL MEASUREMENTS

To study how the fluorescence level of the red plasmid varies with different parameters it was followed a protocol developed by Møller Larsen 2021 and Cordero Sánchez 2021. Single red bacteria were submerged inside semi-solid media where they grow in a three-dimensional colony. An overnight culture was diluted three times by serially diluting 10 μl of the bacterial culture in 1 ml of LB medium. From the final diluted solution 10 μl were poured in a 2 ml Eppendorf tube at 55 $^{\circ}C$ that contains the growth media (M63 Minimal Media or MOPS Minimal Media (see Appendix 10)) + 0.5 % agar, and supplemented with 30 μg/ml kanamycin or without kanamycin and KNO_3 (no KNO_3, $1mM$, $10mM$, or $100mM$ KNO_3). Once the bacteria were submerged in the agar the whole content of the Epperdorf tube was quickly poured into a small Petri dish (see Figure 14). When the agar was solidified the 16 plates were placed in an incubator for 14 h at 37 $^{\circ}C$ and imaged with a Confocal Microscope. All the images were taken under the microscope (see Figure 12A) with the same settings to be able to compare the intensity fluorescence levels.

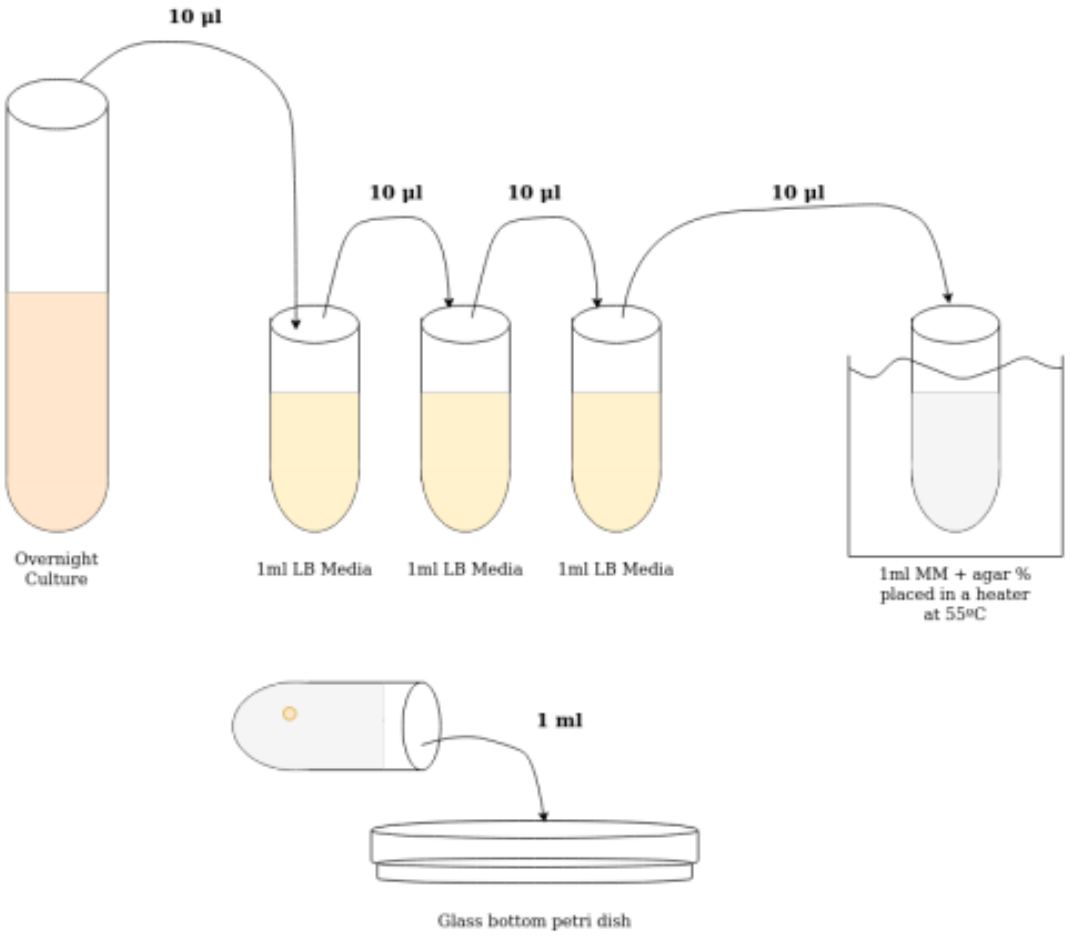

Figure 14: Protocol sketch to grow three-dimensional bacterial colonies forming from one single cell. An overnight cultures is 3 times diluted in LB such that the concentration of bacteria added to the final Eppendorf containing minimal liquid media + 0.5 % agar is 10^{-8} times the concentration of the overnight culture. The Eppendorf containing minimal media + 0.5 % agar is mixed and then poured its content in a glass-bottomed Petri dish. Reprinted from (Cordero Sánchez 2021).

4.7 IMAGE PROCESSING

Once the data was obtained under the same conditions following the protocol, mentioned in section 4.7.1, image processing is required before proceeding to the analysis of the images. First, it is needed to correct drift in the XY plane, probably caused by some movement on the heat stage, and remove the background noise (a video showing the drift in the XY plane can be found on the data repository of reference (Vázquez 2021b)). To correct for the drift it is assumed that the center of mass of the

colonies does not move or change over time. This assumption is reasonable since the bacteria used in these experiments are not motile and do not diffuse through the agar. After determining the center of mass of the colonies, the images were cropped into a new image of dimensions (180x180) pixels with the center of mass of the colonies in the middle of the image. To remove noise from the images an adjustment of *Brightness/Contrast* was first performed. Then, the background noise was removed. The image processing was done using *FIJI* (Schindelin et al. 2012). The image processing steps followed in this project to correct the drift in the XY plane and to remove noise can be summarized as:

1. Adjust *Brightness/Contrast*.

2. With the last t frame (number 21) find the initial and final stacks of the imaged colonies (when the colony starts to fade away). Cut all the frames with the same initial and final Z-stack.

3. Correct the drift in the XY plane by finding the center of mass for each image (*Just Analyze* $>$ *Set Measurements* $>$ *activate Center of mass*) and cut the original image in a new (180x180) pixels image with the center of mass of the colony in the middle of the image.

4. Remove background noise with *Remove outliers*: this is a selective median filter that replaces a pixel by the median of the pixels in the surrounding if it deviates from the median by more than a certain value (Wiki 2019).

Figure 15 shows a Z-projection image of the colony at different points of the image processing steps.

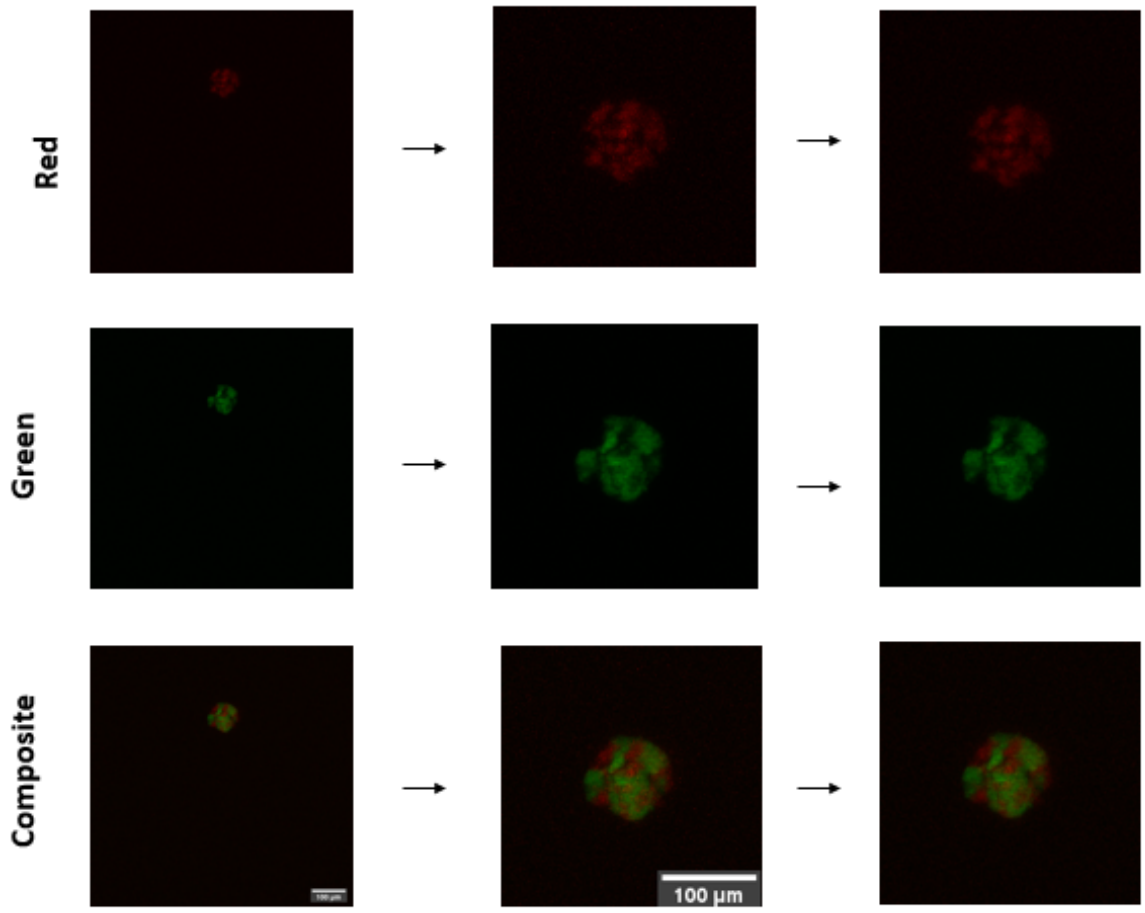

Figure 15: Image processing workflow for the same temporal frame. From top to bottom: red-fluorescence images, green-fluorescence images, and composite images. From left to right: the first column of images shows the raw image without any image processing; the second column shows the same image after cropping it into a new image of dimension (180 x 180) pixels, where the center of mass of the colony is located on the center of the image. The Bright and Contrast of the images were optimized. The last column and last step show the images after subtracting the background noise. The scale is the same for all the images in the same column. The images on the second and third columns have the same scale.

4.7.1 *Segmentation*

In a Confocal Microscope, the imaging depth is limited by scattering and absorption of the emission and excitation light. The excitation light has to penetrate the sample as the focal point moves deeper into the colony, this will produce that the intermediate material between the light source and the focal point will absorb and scatter some of the emission and excitation light. Thus, when we image a colony we are just able to obtain information about its bottom half. This half starts fading as we reach the equator of the colony. Even though the colony fades away it does not imply that the colony ends there. We removed the Z-stacks when the colony starts fading. Figure 16 shows a three-dimensional reconstruction of the colonies for both red and green bacteria before and after the cut-off in the Z-stacks. Segmentation was also required to count the green and red sectors formed on the colony. The segmentation was done using *FIJI* (Schindelin et al. 2012). The followed workflow can be summarized as:

1. Start from the corrected images (lateral drift corrected and noise removed).

2. For each time frame find the initial and final stacks of the imaged colony and remove the rest Z-stacks.

3. Apply an intensity threshold to distinguish the colony from the void. Threshold following the Otsu method (Otsu 1979): binarization algorithm that involves iterating through all the possible threshold values and calculating a measure of spread for the pixel levels on each side of the threshold.

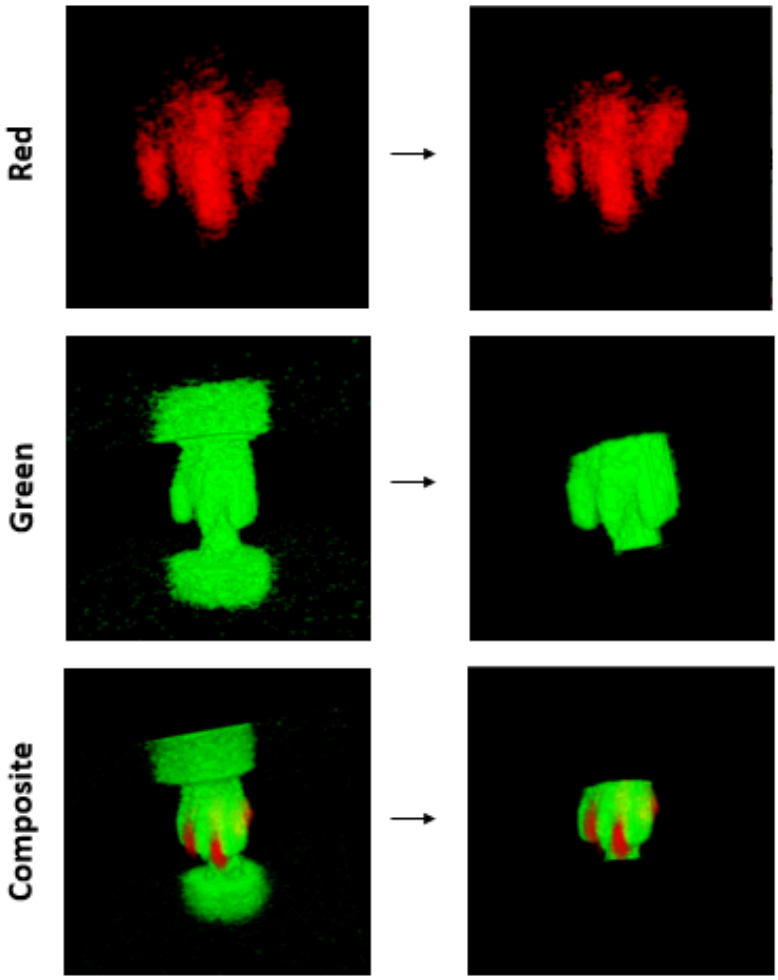

Figure 16: Three-dimensional reconstruction of the colony previously shown in Figure 15. From top to bottom: red-fluorescence images, green-fluorescence images, and composite images. The first and second columns show the colony before and after the cut-off in the Z-stacks, respectively. The three dimensional reconstruction was done using *3D Viewer* plugin (Schmid et al. 2010) on FIJI (Schindelin et al. 2012).

Part IV

RESULTS

5

RESULTS

In nature, bacterial colonies are often comprised of multiple species, and these feature a diverse repertoire of social interactions. These interactions may lead to the emergence of complex spatial structures. So far, most of the experimental studies that shed light on the mechanism behind the pattern formation are done in two dimensions by inoculating bacteria on agar structures. In this thesis, I developed a protocol for growing three-dimensional multi-species bacterial colonies inside a semi-solid media. This three-dimensional setting replicates better what happens in some environmental bacterial habitats. This protocol is based on the methods by Buffi et al. 2011, where they develop a miniaturized bacterial biosensor. In their methods, they encapsulate *E. coli* cells which produce a variant of the green fluorescent protein after contact with arsenite and arsenate in agarose beads and incorporate them into a microfluidic device. Overall, our protocol consists in: mixing at high-speed pluronic acid [1], agarose and a mix of two different strains of bacteria labeled with two fluorescence colors. This mix is added drop by drop into warm silicone oil to form agarose beads and then plunged into a water-ice bath. When plunged into a water-ice bath, the agarose gelates, and solid gel beads form inside the droplets, gluing the bacteria together (Schaerli 2018). These agarose beads provide a spherical scaffold while allowing nutrients and gases to diffuse trough (Bio 2021). They, therefore, display many similarities to the natural environment of living cells. Later, these beads are

1 Pluronic acid is a stabilizer of cell membranes protecting from membrane shearing and additionally acting as an anti-foaming agent.

size-fractionated between 40 and 70 μm. Three-dimensional colonies can grow by submerging the beads inside soft agar and pouring their content in a glass-bottomed Petri dish. These agarose beads remain in a solid gel state even though they are submerged in warm agar and incubate at 37 °C, given that the melting point of the agarose is 65.5 °C (Bio 2021). During incubation, the cells grow into a three-dimensional mixed colony with an intricate patterning that slightly resembles the pattern of the distribution of oceans and continents on the planet Earth.

This chapter contains the obtained results in this thesis and it is mainly divided into five different sections. In section 5.1, we show how we estimated the number of cells we needed to encapsulate inside the agarose beads to have high segregation between our co-cultured strains to observe intricate patterns. In section 5.2, we characterized the toxicity of the main compounds we use to carry the protocol and the size and shape of the agarose beads. In section 5.3, we present the main problem encountered when carrying the experiments and we studied the response the red fluorescent protein has to different media and different concentrations of KNO_3. In section 5.4, we tested the effect that freezing has on the beads. Finally, in section 5.5, we investigated the growth dynamics and the resulting patterning formed on the multi-species three-dimensional colonies.

5.1 ESTIMATING INITIAL CONCENTRATION OF CELLS

As explained in Chapter 3, Van Gestel et al. 2014 showed with an individual-based model in two dimensions that the initial cell density at the onset of the colony growth affects spatial pattern formation. Their simulations clearly revealed that the degree of spatial assortment is closely related to the density of founder cells; the fewer the number of founders, the higher the degree of assortment (Figure 5).

Based on this array-based modeling and other similar models, we assume it is reasonable to expect the same behavior in our thee dimensional setting: at the onset of the colony growth, the green and red founder cells are distributed randomly and separated from each other within the agarose beads. The degree of separation is highest at low initial densities given stronger segregation that gives rise to

the formation of sectors within the colony. This is why we focused our investigation at low initial cell densities, where co-cultured strains stronger segregate in space, resulting in intricate patterns.

To estimate the concentration needed to have high segregation between our co-cultured strains, we established we needed $N \sim 10$ cells/bead so we could make sure the beads would encapsulate the two populations of cells (both green and red) at the same time. Let us consider the beads with the smallest diameter, 40 μm, and therefore the smallest volume, V. Assuming spherical beads, the volume of the beads is given by $V = \frac{4}{3}\pi R^3$, where R is the radius of a bead. For a diameter of 40 μm we get a total volume of $3.35 \cdot 10^{-8}$ ml.

Thus, the initial concentration of cells, C, needed for encapsulating 10 cells inside the volume V is:

$$C = \frac{N}{V} = \frac{10 \text{ cells}}{3.35 \cdot 10^{-8} \text{ ml}} = 3 \cdot 10^8 \text{ cells/ml}.$$

This concentation is obtained by taking 100 μl from an overnight culture of red and green cells, $\sim 10^9$ cells/ml, after growing $\sim$8 h. This measure can be always controlled and determined by measuring its optical density (OD600) with a spectrophotometer [2].

5.2 SYSTEM CHARACTERIZATION

In this section, we explain how the main compounds we use to carry the protocol are toxic. Moreover, the size and shape of the agarose beads was studied.

2 The optical density is a rescaled transmitance, defined as OD600 = - $\log_{10} T(\lambda)$. The density of the sample is measured by passing light at a $\lambda = 600$nm. This wave length is usually used in spectrophotometry to estimate the cell concentration in cultures, since does little or no to damage the sample.

5.2.1 *Component toxicity*

For studying the toxicity of the main components used in the protocol (pluronic acid and silicone oil), we performed a paralleling limiting dilution experiment (Figure 13A) and compared it with a reference of no toxicity. For this, a grown overnight culture of green and red cells ($\sim 10^9$ cells/ml) was ten-fold diluted multiple times in 1 ml of Pluronic acid, Silicone Oil or PBS and then the number of viable cells was determined. Figure 17 shows how the silicone oil is highly toxic for bacterial cells. Just 3 bacterial cells are able to survive from the overnight culture after being diluted in 1 ml of silicone oil. On the other hand, Pluronic acid did not show any sign of toxicity.

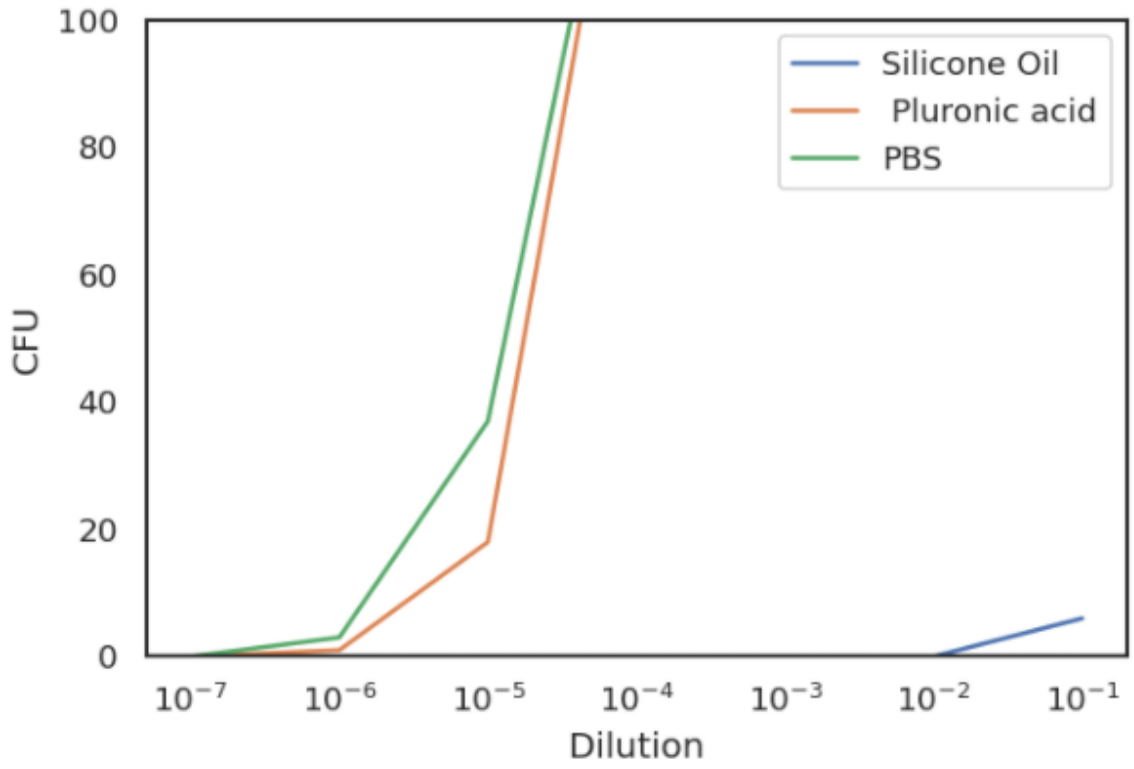

Figure 17: Silicone oil and pluronic acid toxicity. CFU counts as a function of the dilution level in logarithm scale. Seven dilution levels were examined: 10^{-1} - 10^{-7}. The CFU values from 10^{-1}-10^{-5} for pluronic acid and PBS have values larger than 100 CFU.

5.2.2 *Beads shape and size characterization*

In this section, we explain how we investigated the shape and size of the agarose beads. All beads had a spherical form, as expected (Figure 18). These agarose beads are done by adding drop by drop a mix of pluronic acid-agarose-cells in warmed silicone oil. Then this mix is plunged into a water-ice bath to produce the agarose beads (see the protocol in section 4.2). The agarose gelates upon contact with the ice and solid gel beads form inside the droplets (Schaerli 2018). Surface tension is responsible for the shape of liquid droplets. [3]

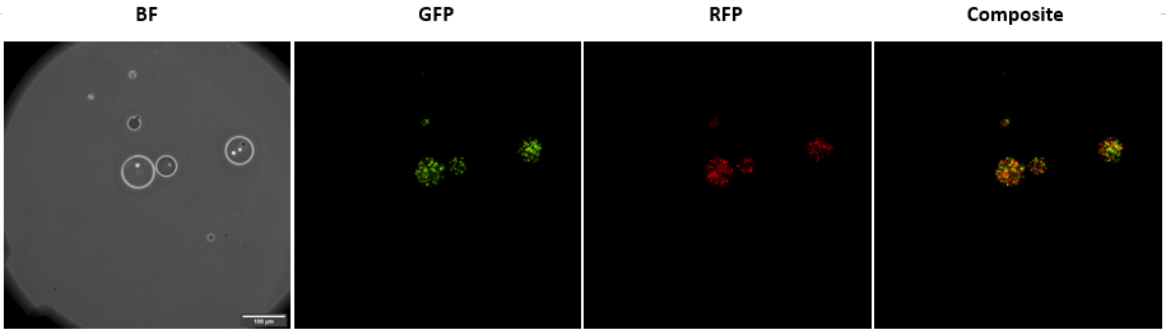

Figure 18: Agarose beads size-fractionated between 40 and 70 μm encapsulating green and red cells. From left to right: bright field images (BF), green-fluorescence images (GFP), red-fluorescence images (RFP), and composite images. The scale bar (100 μm) is equal for all the images.

The diameter of the agarose beads is size distributed between 20 μm and 80 μm. Figure 19 shows the distribution of the bead sizes in micrometers for a sample of 26 beads. The average size of the beads was $(59 \pm 13)\mu$m $(mean \pm SD)$. The diameter of the beads was estimated from images like Figure 18. Moreover, Figure 18 shows how we are able to encapsulate both green and red cells inside the agarose beads. Looking at these beads after some hours shows that these cells are able to grow

3 Surface tension is the tendency of liquid surfaces at rest to shrink into the minimum surface area possible. Due to the cohesive forces, a molecule is pulled equally in every direction by neighboring liquid molecules, resulting in a net force of zero. The molecules at the surface are pulled inward. This creates some internal pressure and forces liquid surfaces to contract to the minimum area and thus acquire a spherical shape.

inside the beads, implying that the agarose scaffold protects the cells from the toxicity of the silicone oil.

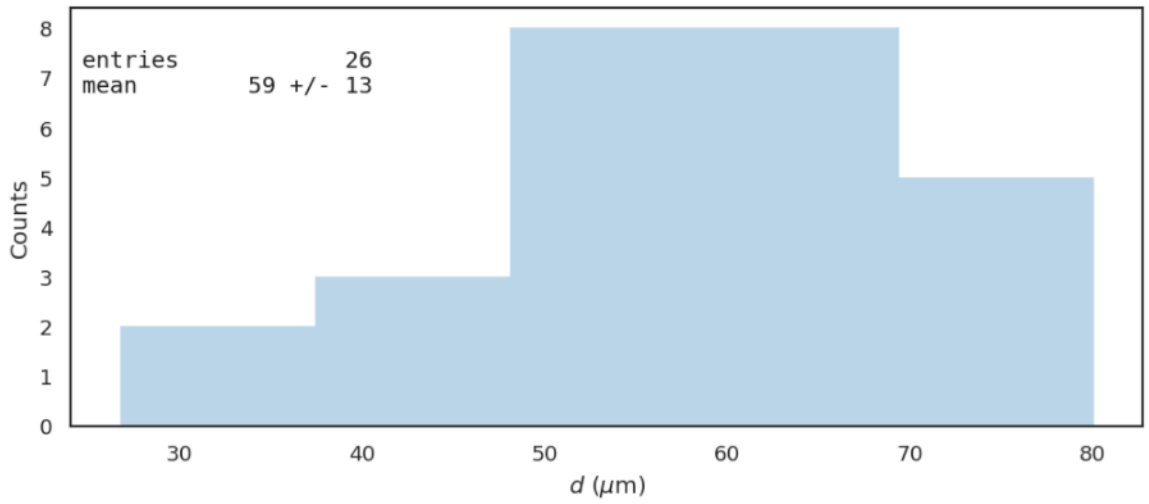

Figure 19: Agarose beads size distribution. The average diameter value of the beads is (59 ± 13) μm $(mean \pm SD)$ for $N = 26$.

5.3 RED FLUORESCENCE LEVELS RESPONSE TO DIFFERENT MEDIA AND DIFFERENT CONCENTRATIONS OF KNO_3

The main obstacle during this thesis was the low fluorescence intensity level of the red fluorescent plasmid. It is known that fluorescent proteins require molecular oxygen for the maturation of fluorescence, which restricts the study of microorganisms in a low-oxygen environment (Landete et al. 2015). Sønderholm et al. 2017 studied bacteria encapsulated in millimiter-sized protanal beads (2 % wt/vol) [4] that formed aggregates ($\sim$100 μm) similar to what is observed in chronic bacterial infections. They found that this aggregate inside the protanal beads is exposed to steep oxygen gradients, with zones of oxygen depletion, and that nitrate may serve as an alternative to oxygen, enabling growth in oxygen-depleted zones. The aggregates formed primarily at the periphery of the beads, but this tendency was alleviated by the addition of the alternative electron acceptor potassium nitrate $100mM$

4 Alginate extracted from the brown alga *Laminaria hyperborea*.

KNO_3. Moreover, Kvich et al. 2019 following the methods of Sønderholm et al. 2017 showed how anoxic conditioning (restriction of molecular oxygen, O_2) generates difficulty to culture bacteria during biofilm growth. Growth difficulty to culture populations was achieved by substituting O_2 with $10mM\ KNO_3$ as an alternative electron acceptor for anaerobic respiration. These suggest that inside our agarose beads could also be zones of oxygen depletion and that potassium nitrate may serve as an alternative to oxygen, which could increase the fluorescence levels of our fluorescent proteins. We decided to investigate two different growth media, M63 Minimal Media and MOPS Minimal Media, supplemented with and without kanamycin for four different concentrations of KNO_3; no KNO_3, $1mM$, $10mM$, and $100mM\ KNO_3$ as a solution to increase the fluorescence level of the red fluorescence plasmid. Figure 20 shows the results of the experiment. The results shown in Figure 20 are very inconclusive and it seems there is no correlation between the level of fluorescence of the red fluorescent protein and the different parameters that we varied on the experiment. The specifications of the plasmid indicate that the plasmid confers resistance to kanamycin 30 μg/ml and that it is needed to supplement the medium where the bacteria grow with 30 μg/ml kanamycin to maintain the plasmid. Nevertheless, Figure 20 shows that the colonies grown in plates without kanamycin are still carrying the plasmid after 14h . This can be explained by the high copy number of the plasmid that, in *E. coli*, is $\sim$500, so it might take time until they lose the plasmid in the absence of kanamycin. This is often the case with this kind of mammalian plasmids. Even though it seems not to be needed to maintain the plasmid during the colony growth we decided to follow the recommendations of the manufacturer and supplement all our medium with 30 μg/ml kanamycin. This also gave us the advantage of being working with cells resistant to kanamycin and at the same time avoid any external contamination. Motivated by the strong arguments discussed by Kvich et al. 2019 and Sønderholm et al. 2017 about the existence of zones of oxygen depletion within their beads, and that nitrate may serve as an alternative to oxygen, we decided to follow Sønderholm et al. 2017 suggestion and supplement our growth plates with $10mM\ KNO_3$. The growth medium chosen for our experiment

was M63 Minimal Medium since it is much easier to elaborate in the laboratory and MOPS medium does not seem to provide any additional advantage.

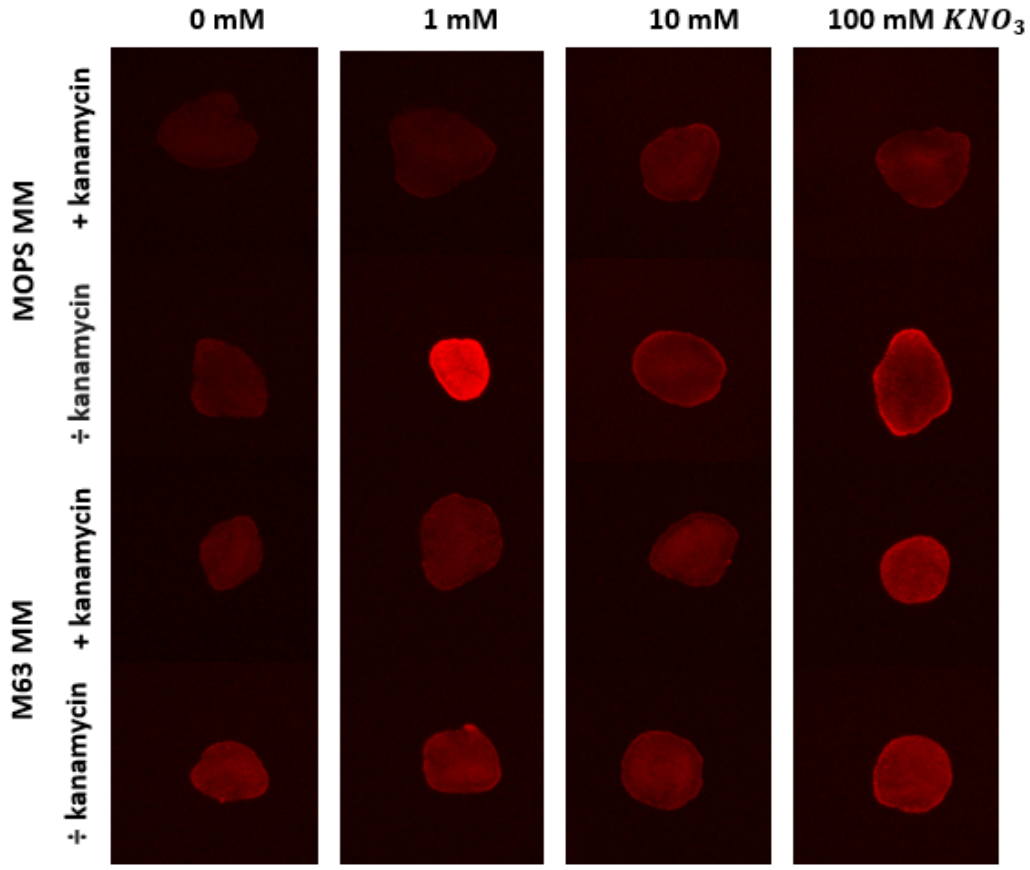

Figure 20: Visual impression of the effect of the fluorescence level on the red fluorescence protein for two different growth mediums (M63 Minimal Media and MOPS Minimal Media), supplemented with and without kanamycin for four different concentrations of KNO_3. From top to bottom: MOPS Minimal Media plates supplemented with 30μg/ml kanamycin, MOPS Minimal Media plates without kanamycin, M63 Minimal Media plates supplemented with 30μg/ml kanamycin, M63 Minimal Media plates without kanamycin. Four different levels of KNO_3 were examined: no KNO_3, $1mM$, $10mM$, or $100mM$ KNO_3.

5.4 EFFECT OF FREEZING THE BEADS

Growing multi-species three-dimensional colonies is very time-lab consuming. The overnight culture takes ∼8 h, the encapsulation process takes ∼2 h, submerging the agarose beads inside soft agar takes ∼30 min. Later, these colonies are incubated for 5 h and imaged during 5 h. To reduce this time and separate the procedure in two different days it was proposed to freeze the beads. We found that the cells inside the beads do not loose viability after being frozen and they behave, in principle, similar as the freshly made beads (Figure 21). We established then that the beads would be done and freeze in a day and, when needed, they would be melted and submerged in soft agar to grow as three-dimensional colonies.

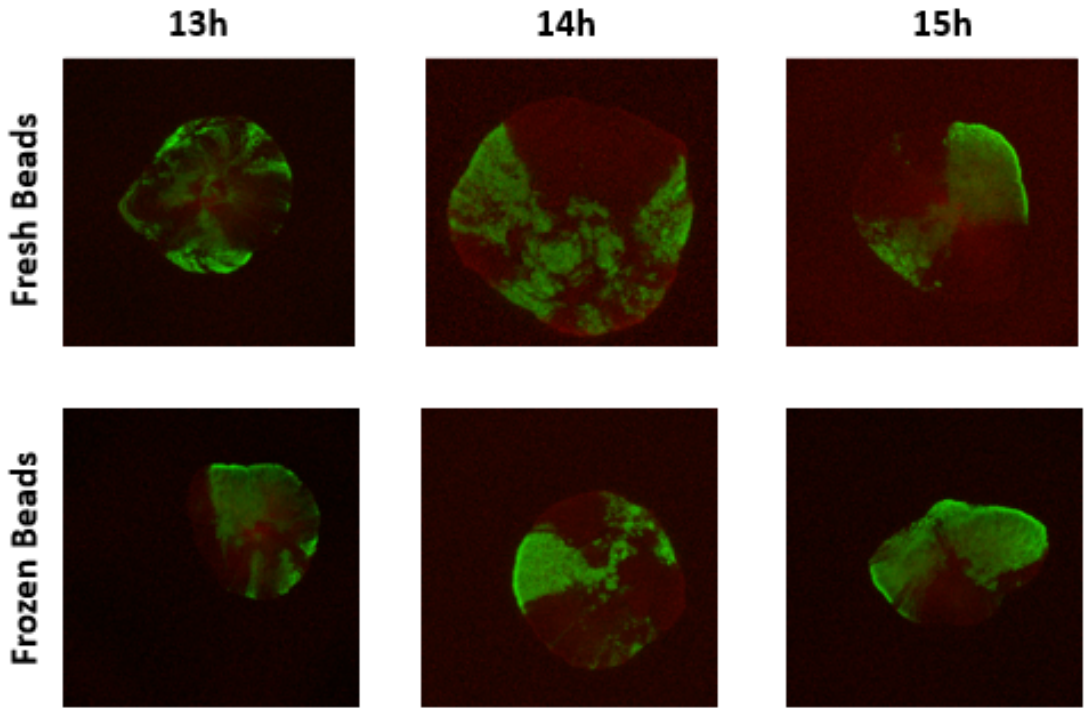

Figure 21: Growth comparison of fresh and frozen beads. The fresh and frozen beads are grown for 13 h , 14 h and 15 h.

5.5 GROWTH DYNAMICS OF THREE-DIMENSIONAL MULTI-SPECIES COLONIES AND PATTERNING FORMATION

In aim of investigating the growth dynamics and the resulting patterning formation of three-dimensional multi-species colonies, we developed a novel protocol (see protocol in section 4.2). Two strains of *E. coli* were tagged with color fluorescence proteins, red or green, to identify whether cell lineages remain randomly mixed or become spatially segregated as cell groups expand. The three-dimensional multi-species bacterial colonies were grown in M63 minimal media with an agar concentration of 0.5 %. The colonies were imaged every 15 min for 5 h after an incubation time of 5 h. The study concluded with 6 samples, each of them containing 21 temporal samples with green and red fluorescence images. This corresponds to a total number of 252 images. The whole dataset can be found on the repository of reference (Vázquez 2021a).

5.5.1 *Growth dynamics of three-dimensional multi-species bacterial colonies*

To study the growth dynamics of multi-species bacterial colonies in three dimensions the evolution of the diameter of the colony was studied over time. The diameter was estimated from the maximum intensity Z-projection of the colonies with *Image J*. We defined the diameter of the colony as the distance from one edge to the other edge of the colony. This measure was repeated four times and the mean and standard deviation of these values was calculated. We estimated the error of each individual measure to be ± 3 pixels for each size, this corresponds to ± 4 μm. Figure 22 shows the growth of one of the colonies over time and the definition of diameter. A video of a three-dimensional multi-species bacterial colony growing can be found in the repository of reference (Vázquez 2021b).

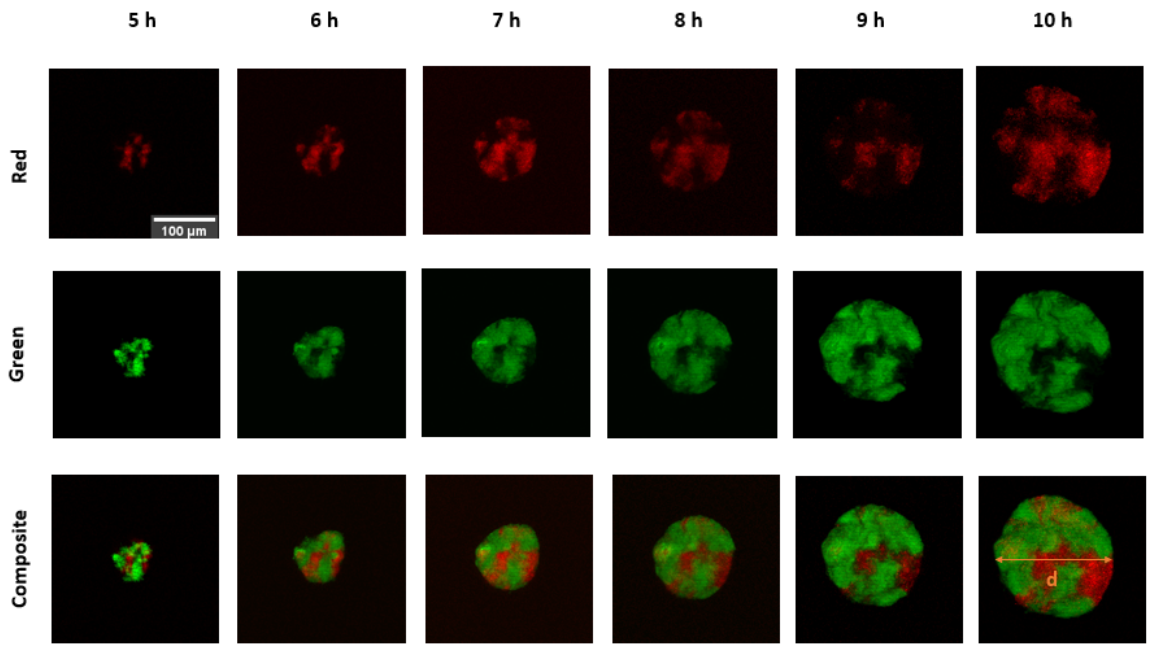

Figure 22: Colony growth of a two-mix color bacterial colony. The images show a maximum intensity Z-projection of the colony growing 5 h on the microscope after 5 h of incubation time. From top to bottom: red-fluorescence image, green fluorescence image and composite image. The scale is the same for all images. The last composite image shows the diameter of the colony.

Figure 23 A shows how the diameter of the colonies evolves over time for the six different samples and its average behaviour. As it can be seen in Figure 23 A there is a window from 6 h to 9 h where the diameter grows linearly over time. However, this linear growth is not necessarily the same for all the colonies (Figure 23 B). However, under $<$6 h the colonies' diameter shows a different tendency. It is believed this is caused by how the cells are distributed inside the colony in a loose way. The colony does not grow as a whole but the green and red clusters are growing separately. We also discard the diameter values from $>$9 h since they are of the order of the agar thickness of the plate.

From 6 h to 9 h the colony diameter grows linearly with time and we can assume the colonies to be densely packed. With these diameter values and assuming spherical symmetry, we can estimate the number of cells within each colony. The number of cells, N, is given by

$$N = \frac{V_{sphere}}{V_{E.\ coli}} \tag{6}$$

where $V_{sphere} = \frac{4}{3}\pi\left(\frac{d}{2}\right)^3$ with d being the diameter of the colony, and $V_{E.\,coli} = (1.19 \pm 0.36)$ μm^3 (Monds et al. 2014). Figure 23 C shows the temporal evolution of the number of cells of the colony for the linear window. Since the diameter grows linearly over time, from Equation 6, the number of cells $N \sim d^3$.

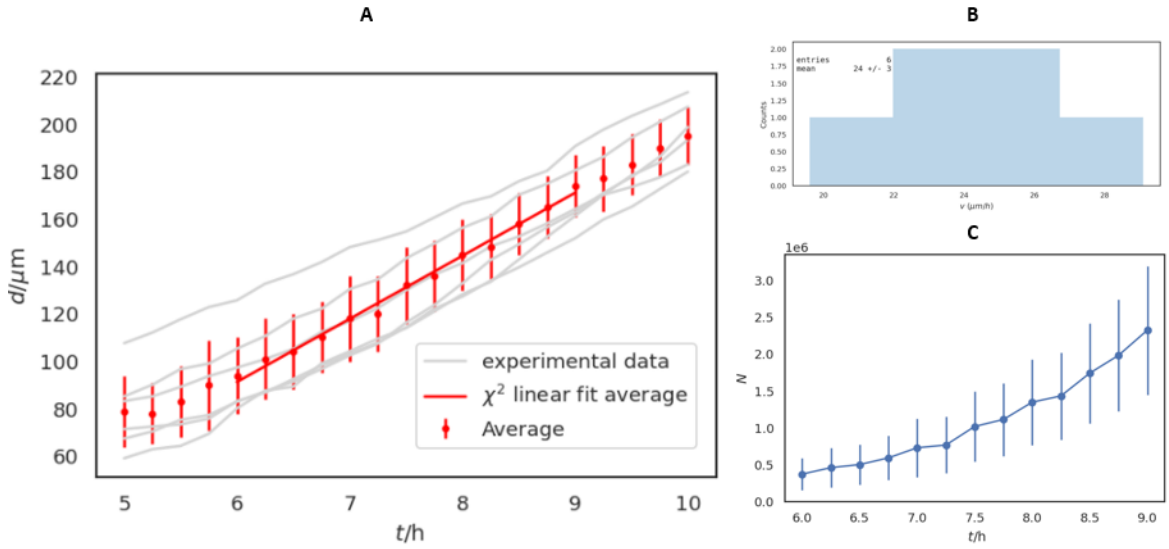

Figure 23: A) Temporal evolution of the diameter of three-dimensional multi-species bacterial colonies. The grey lines correspond to the diameter determined experimentally for the 6 different samples. The red dots and error bars are the average diameter value (mean $\pm$ SD) of all samples. The red line is a χ^2 linear fit for the average diameter values of all the experimental samples. $\chi^2 = 0.27$ for the linear fit. B) Growth rate distribution of the colonies during the linear window. C) Temporal evolution of the number of cells, N, from 6 to 9 h. N grows proportionally to $\sim d^3$.

5.5.2 *Counting sectors in three-dimensional multi-species bacterial colonies*

To investigate how the number of green and red sectors varies over time it was needed to do segmentation and to visualize the colony in three dimensions with a *3D Viewer FIJI* plugin (Schmid et al. 2010); as detailed in section 4.7.1. We define sectors as clusters of red or green cells not connected to another cluster of the same color (Figure 24).

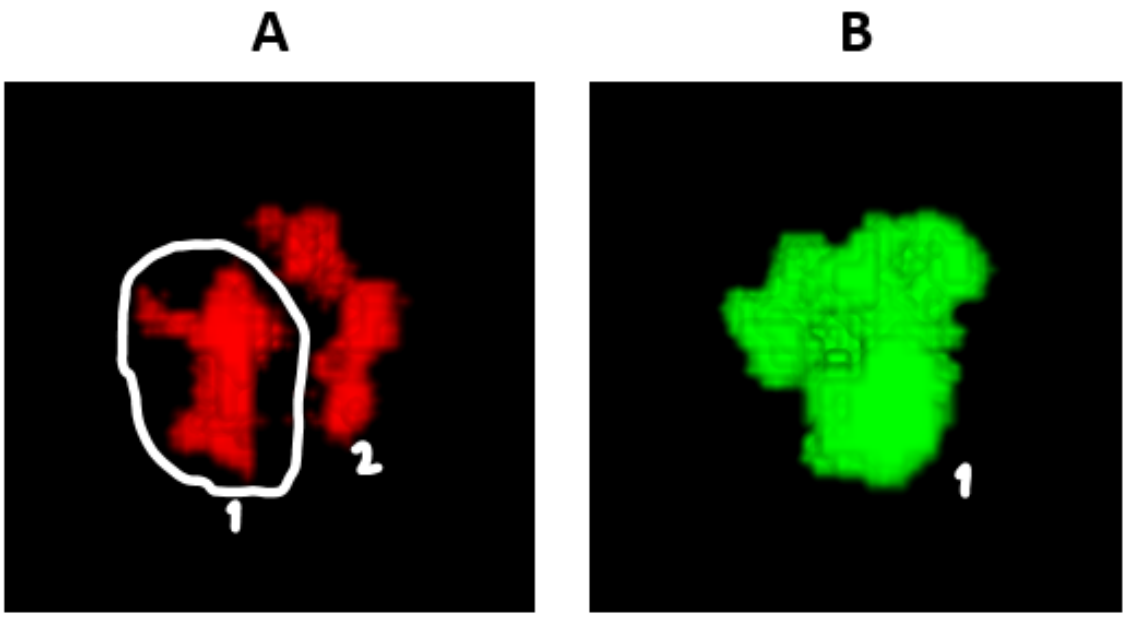

Figure 24: Three-dimensional reconstruction of the green and red cells of the same colony forming sectors. A) Two different red sectors. B) 1 green sector.

Figure 25 shows the evolution of green and red sectors in the colonies over time. On one hand, the number of green sectors is equal to one for all the experiments and, additionally, it remains constant during the 5 h imaged on the Confocal Microscope. On the other hand, the number of red sectors seems to vary slightly more overtime during 5 h to 9 h and after 9 h it seems to stabilize.

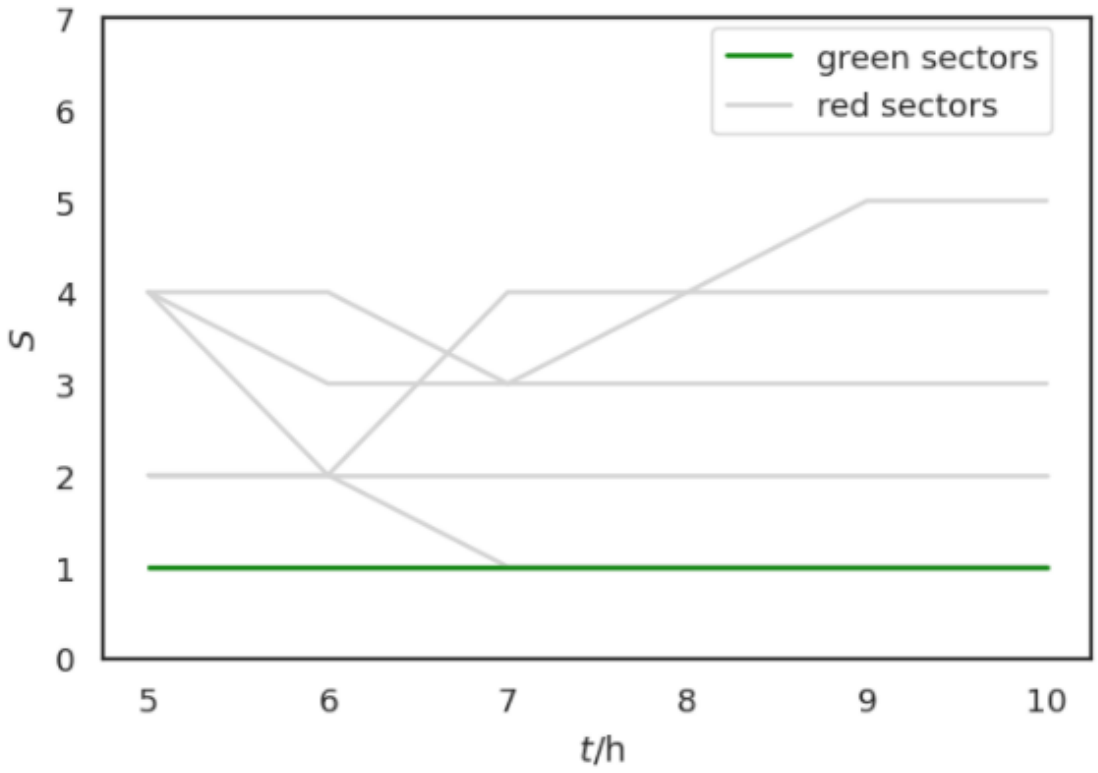

Figure 25: Temporal evolution of the number of green and red sectors. The green and grey lines account for the green and red sector values determined for the 6 experimental samples, respectively.

Figure 26A shows a three-dimensional reconstruction of one of the colonies and its temporal evolution (the colony is the same as in Figure 22). These three-dimensional multi-species colonies display an intricate patterning that slightly resembles the pattern of the distribution of oceans and continents on the planet Earth. The green cells resemble the continents and the red cells the oceans. Our results are comparable with the results obtained when simulating the colony growth initiated with more than 10 cells both red and blue with an Eden Model. Figure 26B shows the results of the Eden Model simulations [5], where each color cell was restricted to grow to the same color as it self. A video of the results of the Eden Model simulations can be found on the repository of reference (Vázquez 2021b).

5 The simulation image was provided by Martin Møller Larsen.

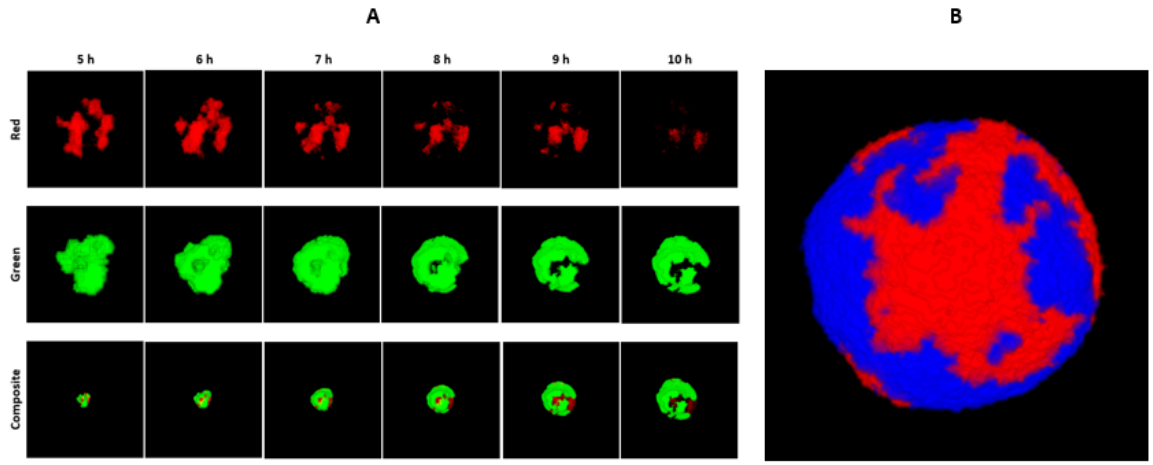

Figure 26: Three-dimensional reconstruction of multi-species colonies forming a planet earth-like patterning after growing. A) Colony growth of the colony shown in Figure 22. From top to bottom: red-fluorescence images, green fluorescent images and composite images. B) Eden Model simulation of a colony growing from a few blue and red founder cells.

Part V

DISCUSSION

6

DISCUSSION

In this thesis, we wanted to investigate the growth dynamics and the resulting patterning formation of three-dimensional multi-species colonies in order to understand how and why different genotypes arrange themselves in space as cells grow and divide. For this, I developed a novel protocol that allows the growth of three-dimensional mixed-species colonies. This is done by encapsulating bacteria carrying a red or green tags inside a spherical scaffold made of agarose that allows the diffusion of nutrients and gases inside. Three-dimensional colonies can grow by submerging these beads inside soft agar and pouring their content in to a glass-bottomed Petri dish. So far, experimentally these mixed-species colonies were only studied in two dimensions. In two dimensions, this is done by inoculating a droplet containing a mix of bacteria on hard agar surfaces. In these surface-attached colonies, cell division is often restricted to the edge since cells at the edge of a colony can access more nutrients than cells in the center. As a consequence, growth is characterized by expanding frontiers of diving cells (Hallatschek et al. 2007) and results in the emergence of sectors.

The main obstacle found during this thesis was the low fluorescence level of the red fluorescent protein. One possible reason could be the lack of oxygen inside the beads. Fluorescent proteins need oxygen for the maturation of fluorescence, so it was believed that the addition of the alternative electron acceptor potassium nitrate would serve as an alternative to oxygen within the beads and this would increase the fluorescence levels (Sønderholm et al. 2017; Kvich et al. 2019). However, our results were very inconclusive and we did not find any proofs this oxygenation increased the

fluorescence levels of our red fluorescent protein (Figure 20). In future work, to ensure quantitative measurements and high spatial precision, it is needed to replace this plasmid with another with higher fluorescence intensity. In order, to choose the correct plasmid we have to take into account many variables, both intrinsic and extrinsic to the fluorescence proteins since they might influence their brightness when expressed in bacterial cells. For instance, fluorescence proteins are often undesirably sensitive to intracellular conditions such as pH and ion concentration (Morikawa et al. 2016).

Beginning with a few cells tagged with two different colors inside agarose beads and submerged in soft agar, the growth and division of cells over time results in an emergent colony pattern that slightly resembles the pattern of the distribution of oceans and continents on the planet earth. This system presents many different biological and physical questions: how and why different genotypes arrange themselves in space as cells grow and divide? Here, we investigated the growth dynamics and the resulting intricate patterning these colonies formed. To do so, we studied how the diameter of the colony evolved over time. We found the colonies emerging from agarose beads have a window where they grow linearly. The average behavior of these mixed three-dimensional colonies behaves linearly in a window of $\sim$3 h, from 6 h to 9 h of growth (Figure 23A). However, this linear growth is not necessarily the same for all the colonies (Figure 23B). This discrepancy in the growth rates for the individual experiments can be explained by the differences in the number of cells inside the beads, fewer cells inside the beads for the same nutrient amount could result in a faster division rate (Shao et al. 2017). This linear growth can be understood as if the growth of cells was restricted to the outer parts of the colony. Bacteria in the center of the colony might starve due to insufficient nutrient penetration as the colony becomes bigger (Kuennen and C. Wang 2008). Motivated by previous lattice models, where the radius of the colonies scales linearly with time, $R \propto t$ (Kuennen and C. Wang 2008) we propose to focus future investigations on the study of three-dimensional multi-species bacterial colonies emerging from cells inside agarose beads within this linear growth region, where the colony may be densely packed. On the other hand, growth under 6 h appears to be slower. This may be caused due to the low connectivity of the cells inside and outside the beads, resulting in not-connected

clusters of bacteria growing separately instead of as an unified colony. Furthermore, from >9 h the colony has again a slower rate of growth. I speculate that, as the colony size is quite big and of the order of the agar thickness, this may create stiff gradients of food and oxygen within the colonies and thus the cells within the colony may grow at different rates.

To characterize the emerging pattern we studied how the number of green and red sectors evolved. We observed that the number of green sectors remained constant during the 5 h studied in this project. However, the number of red sectors varied slightly more over time, but still not a lot (Figure 25). To understand these findings, we can think about how the patterns are formed in two dimensions. In two dimensions, the development of well-mixed populations of two fluorescently labeled strains is well-defined. They form sector-like regions with fractal boundaries. The observed genotype distributions can be partitioned into areas of two very different patterns. The central region exhibits a dense speckle pattern, reminiscent of the homogeneous and well-mixed initial population. This region is bounded to a ring of higher speckle density, formed at the edge of the initial droplet. From this ring towards the boundary of the mature colony, the population segregates into single-colored domains. A large number of differently labeled flares radiate and gradually coalesce into a few large sectors that reach the edge of the mature colony (Figure 4A). Additionally, behind the population front there is no noticeable temporal change in the arrangement of the genotypes in space as cells grow and divide (Hallatschek et al. 2007). This made us think, we were looking at our colonies in the period where the pattern was already formed and well established and, as in two dimensions, there was no temporal change in the number of sectors already formed.

Finally, our experimental results align with the results of previous models. With an Eden Model when tracking in time the positions and state of bacterial cells after being grown until the number of cells reaches $\sim 10^6$, the radius of the colony scales linearly with time. Moreover, when simulating the growth of three-dimensional multi-species colonies the outcome also results in a colony with a planet-Earth like pattern when the colonies emerge from >10 cells (Figure 26B).

Part VI

CONCLUSION AND FUTURE WORK

7

CONCLUSION

Understanding the principles governing the formation, structure, and functioning of microbial communities is one of the major challenges in microbial ecology (Dubey et al. 2021). To investigate the growth dynamics and patterning formation of a setting that resembles some ecological systems' bacteria habitats, I developed a protocol that allows growing three-dimensional multi-species bacterial colonies.

With these methods, we measured the growth of the colonies and identified different visible green and red sectors in the bacterial colonies. We found these three-dimensional multi-species colonies emerging from agarose beads have a window where they grow linearly. This indicates that in three-dimensional multi-species colonies the growth of cells might be restricted to the outer parts of the colony, while the center is static. Moreover, we also found in the range time studied in our experiment the number of sectors is well established and remains constant over time.

Finally, we propose that the protocol developed here can be used as a baseline to address these questions of generality with other bacteria, and media. Moreover, the protocol could be used to bring some light to many different biological and physical questions which are not still answered. For instance, this system would be perfect to study the social interactions arising within three-dimensional bacterial colonies comprised of bacteria of the same or different species. Moreover, this system would be as well an excellent tool to study horizontal gene transfer in three dimensions and to establish a framework for understanding the mechanism behind it.

8

FUTURE WORK

The experimental setup used in this thesis proved to have some limitations to acquire data with higher resolution. To overcome these constraints it will be needed to work with cells that carry proteins with higher fluorescence levels. In future work, we should also focus on the linear windows where the colony is assumed to be densely packed.

Imaging methods allowing for detection of single cells combine with deep imaging will allow looking inside the beads and have a full understanding of the colony structure.

Finally, it is worth mentioning some other applications this novel protocol could be used to. It has been theorized, as discussed in Chapter 3, that social interactions in communities would be prevailingly negative except among closely related genotypes. This system would be perfect to study the social interactions arising within three-dimensional bacterial colonies comprised of bacteria of the same or different species. To understand the positive or negative social interactions in play of these evolving colonies it would be useful to compare the mix-color three-dimensional colonies with agarose beads containing just one kind of population's founders. This system would be as well an excellent tool to study horizontal gene transfer in three dimensions and to establish a framework for understanding the mechanism behind it. This could be done based on previous research in two dimensions as Cooper et al. 2017. Understanding how bacteria thrive in competitive habitats and their cooperative strategies for surviving extreme stress can be instructive, for instance, to inspire new

hypotheses and investigations for developing a more rational approach for battling pathogenic bacteria resistant to antibiotics.

Part VII

APPENDICES

9

PLASMIDS

9.1 MAXGFP

maxGFP is a newly discovered green fluorescent protein derived from the copepod *Pontellina sp*. It is characterize for having high fluorescence which makes *maxGFP* ideal for fluorescence microscopy (Addgene 2006).

9.1.1 *Vector description*

pmaxCloning Vector is an eukaryotic expression plasmid to promote constitutive expression of cloned DNA inserts in mammalian cells. The *pmaxCloning* Vector backbone contains immediate early promoter of cytomegalovirus (*PCMV IE*) for protein expression, a chimeric intron for enhanced gene expression and the *pUC* origin of replication for propagation in *E. coli*. The multiple cloning site (*MCS*) is located between the *CMV* promoter and the *SV40* polyadenylation signal (*SV40 poly A*). The *pmaxCloning* Vector must be co-transfected with an expression vector containing a selectable gene for mammalian cells (Lonza 2002). Figure 27 shows the Vector Sequence of *pmaxCloning*. It is characterize for having a high expression rate in mammalian cells, license-free use for research purposes and a multiple cloning site for convenient insertion of the gene of interests, in our case, GFP.

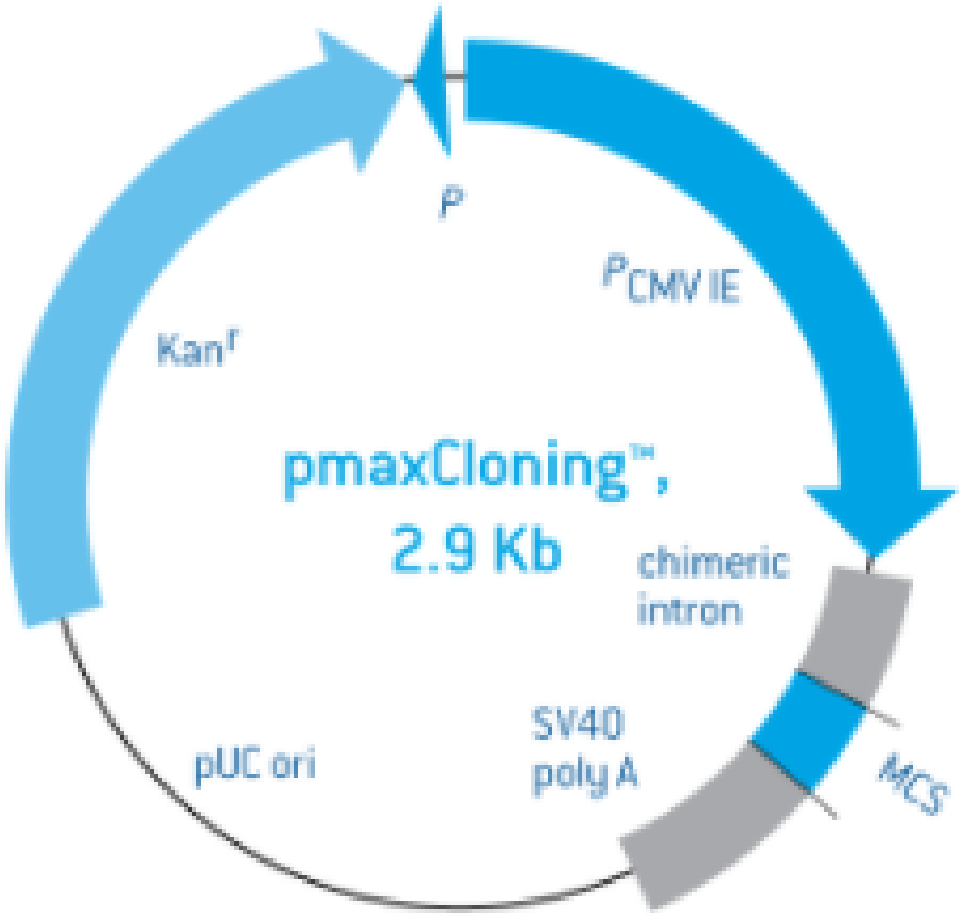

Figure 27: *pmaxCloning* Vector Sequence. The *pmaxCloning* Vector backbone contains immediate early promoter of cytomegalovirus (*PCMV IE*) for protein expression, a chimeric intron for enhanced gene expression and the *pUC* origin of replication for propagation in *E. coli*. The multiple cloning site (*MCS*) is located between the *CMV* promoter and the *SV40* polyadenylation signal (*SV40 poly A*). Reprinted from (Lonza 2002)

.

9.1.1.1 *Cloning of DNA insert*

The *pmaxCloning* Vector does not contain an ATG initiation codon. A translation initiation sequence must be incorporated if the DNA fragment to be cloned does not have an initiating ATG codon or an optimal sequence for initiating translation,

9.1.1.2 *Expression in mammalian cells*

pmaxCloning Vector can be transfected into mammalian cells by any know transfection method. The *CMV* promoter provides strong, constitutive expression of the cloned DNA insert in many cell types.

9.1.1.3 *Propagation in E. coli*

Suitable host strains for propagation in *E. coli* include *DH5alpha*, *HB101*, and other general purpose strains. Plasmid incompatibility group is *pMB1/ColE1.* The vector confers resistance to kanamycin to 30 μg/ml to E. coli hosts. The *E. coli* replication origin is *pUC*. Copy number in E. coli is about 500.

9.2 TURBORFP

TurboFPs are fluorescent proteins characterized by very fast maturation. These proteins are recommended for applications requiring fast appearance (Evrogen 2002a).

9.2.1 *Vector description*

We do not know if the vector used in this thesis is *pTurboRFP-C* vector or *pTurboRFP-N*. In this section we will describe both. All the information can be found in (Evrogen 2002b; Evrogen 2002c).

pTurboRFP-c and *pTurboRFP-N* are mammalian expression vectors encoding red (orange) fluorescent protein *TurboRFP*. *pTurboRFP-C* vector allows generation of fusion to the *pTurboRFP*

C-terminus and expression of *TurboRFP* fusion or *TurboRFP* alone in eukariotic (mammalian) cells while *pTurboRFP-N* does it in the *TurboRFP* N-terminus.

TurboRFP codon usage is optimized for high expression in mammalian cells. Multiple cloning site is located between *TurboRFP* coding sequence and *SV40* polyadenylation signal (*SV40 poly A*) for *pTurboRFP-c*. The Multiple closing site is located between the early promoter of *cytomegalovirus* (*PCMV IE*) and *TurboRFP* coding sequence. The vector backbone contains immediate early promoter of *cytomegalovirus* (*PCMV IE*) for protein expression, *SV40* origin for replication in mammalian cells expressing *SV40* T-antigen, *pUC* origin of replication for propagation in *E. coli*, and f1 origin for single-stranded DNA production. *SV40* polyadenylation signal (*SV40 poly A*) direct proper processing of the 3'-end of the reporter mRNA. *SV40* early promoter (*PSV40*) provides neomycin resistance gene expression to select stably transfected eukaryotic cells using *G418*. Bacterial promoter (*P*) provides kanamycin resistance gene expression in *E. coli*. Figure 28 shows the vector sequence of *pTurboRFP-C* and *pTurboRFP-N*.

9.2.1.1 *Generation of TurboRFP fusion proteins*

A localization signal or a gene of interest can be cloned into multiple cloning site of the vector. It will be expressed as a fusion to the *TurboRPF* C- terminus for *pTurboRFP-C*, or when *TurboRPF* N-terminus for *pTurboRFP-N*, when inserted in the same reading frame as *TurboRPF* and no in-frame stop codons are present. For *pTurboRPF-N* the inserted sequence should contain an initiating ATG codon. *TurboRPF*-tagged fusions retain fluorescent proteins of the native protein allowing fusion localization in vivo. Unmodified vector will express *TurboRPF* whem transfected into eukaryotic (mammalian) cells.

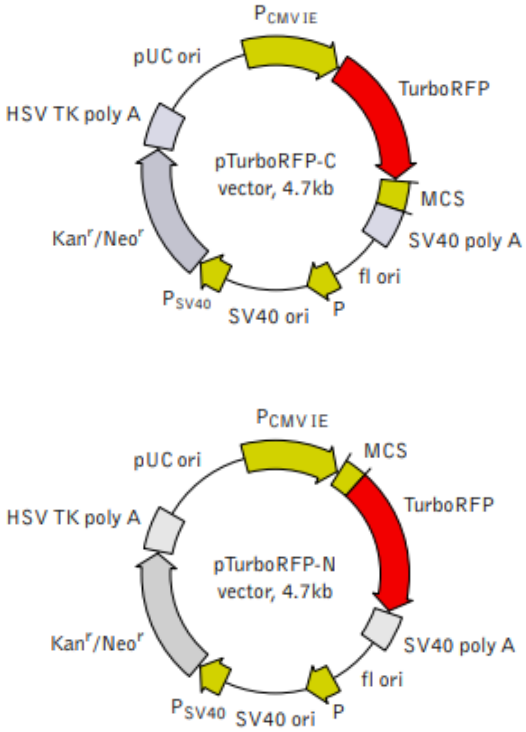

Figure 28: From the top to the bottom: Vector sequence of *pTurboRFP-C* (Reprinted from (Evrogen 2002b)) and vector sequence of *pTurboRFP-N* (Reprinted from (Evrogen 2002c)). The vector backbone contains immediate early promoter of *cytomegalovirus* (*PCMV IE*) for protein expression, *SV40* origin for replication in mammalian cells expressing *SV40* T-antigen, *pUC* origin of replication for propagation in *E. coli*, and f1 origin for single-stranded DNA production. *SV40* polyadenylation signal (*SV40 poly A*) direct proper processing of the 3'-end of the reporter mRNA. *SV40* early promoter (*PSV40*) provides neomycin resistance gene expression to select stably transfected eukaryotic cells using *G418*. Bacterial promoter (*P*) provides kanamycin resistance gene expression in *E. coli*.

9.2.1.2 *Expression in mammalian cells*

pTurboRFP-C, and *pTurboRFP-N*, vector can be transfected into mammalian cells by any know transfection method. The *CMV* promoter provides strong, constitutive expression of *TurboRFP* or its fusions in eukariotic cells.

9.2.1.3 *Propagation in E. coli*

Suitable host strains for propagation in *E. coli* include *DH5alpha*, *HB101*, *XL1-Blue*, and other general purpose strains. Plasmid incompatibility group is *pMB1/ColE1*.The vector confers resistance to kanamycin to 30 μg/ml to E. coli hosts. Copy number in E. coli is about 500.

10

MEDIA PREPARATION

10.1 LYSOGENIC BROTH: RICH MEDIA

Protocol for preparing 100 ml of LB media.

Materials

- *Milli-Q water*
- *Bacto Tryptone*
- *Yeast extract*
- *NaCl*
- *NaOH*
- Plastic dropper pipette
- Kanamycin

1. In a glass bottle pour 100 ml of Milli-Q water and mix the following components in sequence:
    - 1 g *Bacto Tryptone*

- 0.5 g *Yeast extract*
- 0.5 g *NaCl*

2. Check that the pH of the solution is equal to 7. If its smaller adjust the pH value by adding *NaOH* [1] with a dropper pipette.
3. Label the bottle of the solution with a paper for autoclave sterilization. Write your name, date and contain of the solution.
4. Autoclave the solution.
5. If kanamycin antibiotic is needed it needs to be added when the solution has cool down at $\sim$55 °C.
6. Store at room temperature. If kanamycin was added store in the fridge.

10.2 M63 MINIMAL MEDIA

Protocol for preparing 5ml M63 media.

Materials

- 15 ml Falcon tube
- 5x*M63* salt
- 1 mg/ml *B1* stock solution
- 1M $MgSO_4$

1 *NaOH* is the fomula for the inorganic compound sodium hydroxide. Sodium hydroxide raise pH to near neutral when injecting into a solution.

- 20 % w/v *glucose*

1. In a sterilize plastic falcon tube mix the following components in sequence:
    - 5 ml of 5x*M63* salt
    - 25 μl of 1 mg/ml *B1* stock solution
    - 50 μl of 1M $MgSO_4$
    - 250 μl of 20 % w/v *glucose*
2. Store at room temperature.

10.3 MOPS MINIMAL MEDIA

Protocol for preparing 5 ml 5x*MOPS*.

Materials

- 15 ml Falcon tube
- *MOPS*
- 1.2 M K_2HPO_4
- 0.276 M K_2SO_4
- 20 % w/v *glucose*
- *Milli-Q water*

1. In a sterilize plastic falcon tube mix the following components in sequence:
    - 2.5 ml of *MOPS*

- 27.5 μl of 1.2 M K_2HPO_4
- 25 μl of 0.276 M K_2SO_4
- 250 μl of 20 % w/v *glucose*

2. Fill with *Milli-Q water* until reaching 5 ml.

3. Store at room temperature.

11

BACTERIAL CULTURE

MATERIALS

- Bacterial plates with red and green cells (see Appendix 11
- Wooden sticks
- *LB* + 30 μg/ml kanamycin
- 15 ml test tube
- 5 ml glass pipettes

METHOD

1. Take a 15 ml falcon tube for each strain. Label each falcon tube with your name, date, and strain's name.
2. Fill it with 2 ml of LB supplemented with 30 μg/ml kanamycin using a sterile pipette.
3. Transfer one colony from the bacterial plate to each flask using a wooden stick.
4. Incubate for $\sim$8 h at 37°C and 225 rpm. The cap should be open to allow oxygenation.

12

BACTERIAL PLATE

Protocol to obtain bacterial plates with the red and green cells. With this traditional technique of streaking frozen stocks onto a solid medium, one can select for colonies originating from, in theory, a single bacterium. Subsequently, colonies are selected and used to inoculate liquid cultures. Plates last approximately one month.

MATERIALS

- Big plastic petri dish
- *LB*) medium with 1.5 % agar (see Appendix 10)
- Bacterial frozen stocks (green and red cells)
- Wooden sticks
- Kanamycin

METHOD

Pour the agar plates

To prepare solid plates used to prepare streak plates it was added 1.5 % agar percentage (1.5 g of agar per 100 ml of media) to the LB nutritional media.

1. Write your initials, the content and the date on the bottom of the petri dish.
2. Melt the bottle of *LB* + 1.5 % agar in the microwave. Approximately it takes 30 s.
3. When the bottle can be hold with the hand add 30 μg/ml kanamycin.
4. Mix and pour the media into a big petri dish.
5. Let the plate rest overnight undisturbed on the laboratory bench.

Streak the cells

To be certain that you are starting from a single clonal population of cells you need to streak the plates. Repeat the process for each strain. Since both green and red strains have the same growth conditions the cultures can be grown on the same agar plate.

1. Label the plate by writing down your name, data, strain name and fluorescence color.
2. Take a droplet of bacterial from the frozen stock onto the plate using a wooden stick.
3. Streak the droplet onto the plate. Streak in 3 different directions each with a different stick.
4. Put the plate in the incubator and let the colony grow overnight ($\sim$12 h) at 37°C. The agar must be on top to avoid condensed water to fall to the bacteria.

BIBLIOGRAPHY

Addgene (2006). *pMax-E2F1 (Plasmid 16007)*. URL: https://www.addgene.org/16007/.

Allen, Rosalind J and Bartlomiej Waclaw (2018). "Bacterial growth: A statistical physicist's guide". In: *Reports on Progress in Physics* 82.1, p. 016601.

Ben-Jacob, Eshel, Inon Cohen, and Herbert Levine (2000). "Cooperative self-organization of microorganisms". In: *Advances in Physics* 49.4, pp. 395–554.

Bio, Dolomite (June 2021). *Encapsulation of Cells in Agarose: Dolomite Bio Technology*. Accessed: 2021-07-4. URL: https://www.dolomite-bio.com/applications/agarose-encapsulation/.

Bonachela, Juan A et al. (2011). "Universality in bacterial colonies". In: *Journal of Statistical Physics* 144.2, pp. 303–315.

Bramhachari, Pallaval Veera (2019). *Implication of quorum sensing system in biofilm formation and virulence*. Springer.

Buffi, Nina et al. (2011). "Development of a microfluidics biosensor for agarose-bead immobilized Escherichia coli bioreporter cells for arsenite detection in aqueous samples". In: *Lab on a Chip* 11.14, pp. 2369–2377.

Burmølle, Mette et al. (2014). "Interactions in multispecies biofilms: do they actually matter?" In: *Trends in microbiology* 22.2, pp. 84–91.

Cooper, Robert M, Lev Tsimring, and Jeff Hasty (2017). "Inter-species population dynamics enhance microbial horizontal gene transfer and spread of antibiotic resistance". In: *Elife* 6, e25950.

Cordero Sánchez, Mireia (2021). "Study of three-dimensional bacterial colonies: how expression of motility and adhesion factors control colony morphology". MA thesis.

Dubey, Manupriyam et al. (2021). “Environmental connectivity controls diversity in soil microbial communities”. In: *Communications biology* 4.1, pp. 1–15.

Eden, Murray et al. (1961). “A two-dimensional growth process”. In: *Proceedings of the fourth Berkeley symposium on mathematical statistics and probability*. Vol. 4. University of California Press Berkeley, pp. 223–239.

Evrogen (2002a). *Evrogen TurboFPs*. Accessed: 2021-07-4. URL: http://evrogen.com/products/TurboColors.shtml.

Evrogen (2002b). *pTurboRFP-C*. Accessed: 2021-07-27. URL: https://evrogen.com/products/vectors/pTurboRFP-C/pTurboRFP-C.shtml.

Evrogen (2002c). *pTurboRFP-N*. Accessed: 2021-07-27. URL: https://evrogen.com/products/vectors/pTurboRFP-N/pTurboRFP-N.shtml.

Flemming, Hans-Curt et al. (2016). “Biofilms: an emergent form of bacterial life”. In: *Nature Reviews Microbiology* 14.9, p. 563.

FPbase (July 2021). *FPbase Fluorescence Spectra Viewer*. http://www.fpbase.org/spectra/. Accessed: 2021-07-5.

Griffin, Ashleigh S, Stuart A West, and Angus Buckling (2004). “Cooperation and competition in pathogenic bacteria”. In: *Nature* 430.7003, pp. 1024–1027.

Hallatschek, Oskar et al. (2007). “Genetic drift at expanding frontiers promotes gene segregation”. In: *Proceedings of the National Academy of Sciences* 104.50, pp. 19926–19930.

Hibbing, Michael E et al. (2010). “Bacterial competition: surviving and thriving in the microbial jungle”. In: *Nature reviews microbiology* 8.1, pp. 15–25.

Humagain, Sushil (Aug. 2018). *Growth of bacteria and the bacterial growth curve*. URL: https://onlinesciencenotes.com/growth-of-bacteria-and-the-bacterial-growth-curve/.

Jonkman, James et al. (2020). “Tutorial: guidance for quantitative confocal microscopy”. In: *Nature protocols*, pp. 1–27.

Kuennen, Eric W and CY Wang (2008). “Off-lattice radial Eden cluster growth in two and three dimensions”. In: *Journal of Statistical Mechanics: Theory and Experiment* 2008.05, P05014.

Kvich, Lasse et al. (2019). “Oxygen restriction generates difficult-to-culture P. aeruginosa”. In: *Frontiers in microbiology* 10, p. 1992.

Landete, José M et al. (2015). “Use of anaerobic green fluorescent protein versus green fluorescent protein as reporter in lactic acid bacteria”. In: *Applied microbiology and biotechnology* 99.16, pp. 6865–6877.

Lenski, Richard E et al. (1991). “Long-term experimental evolution in Escherichia coli. I. Adaptation and divergence during 2,000 generations”. In: *The American Naturalist* 138.6, pp. 1315–1341.

Lichtman, Jeff W and José-Angel Conchello (2005). “Fluorescence microscopy”. In: *Nature methods* 2.12, pp. 910–919.

Lonza (2002). *Lonza pmax Cloning Vector*. http://bioscience.lonza.com/lonza_bs/DK/en/Transfection/p/000000000000191671/pmaxCloning-Vector. Accessed: 2021-07-4.

Møller Larsen, Martin (2021). “The shape of three dimensional bacterial colonies”. MA thesis.

Monds, Russell D et al. (2014). “Systematic perturbation of cytoskeletal function reveals a linear scaling relationship between cell geometry and fitness”. In: *Cell reports* 9.4, pp. 1528–1537.

Morikawa, Takamitsu J et al. (2016). “Dependence of fluorescent protein brightness on protein concentration in solution and enhancement of it”. In: *Scientific reports* 6.1, pp. 1–13.

Nadell, Carey D, Knut Drescher, and Kevin R Foster (2016). “Spatial structure, cooperation and competition in biofilms”. In: *Nature Reviews Microbiology* 14.9, pp. 589–600.

Nadell, Carey D, Kevin R Foster, and Joao B Xavier (2010). “Emergence of spatial structure in cell groups and the evolution of cooperation”. In: *PLoS computational biology* 6.3, e1000716.

Otsu, Nobuyuki (1979). “A threshold selection method from gray-level histograms”. In: *IEEE transactions on systems, man, and cybernetics* 9.1, pp. 62–66.

Parker, Nina et al. (2018). *Microbiology: OpenStax*.

Pelc, Radek, Wolfgang Walz, and J Ronald Doucette (2020). *Neurohistology and Imaging Techniques*. Springer, pp. 201–223.

Schaerli, Yolanda (2018). "Bacterial microcolonies in gel beads for high-throughput screening". In: *Bio-protocol* 8.13.

Schindelin, Johannes et al. (2012). "Fiji: an open-source platform for biological-image analysis". In: *Nature methods* 9.7, pp. 676–682.

Schmid, Benjamin et al. (2010). "A high-level 3D visualization API for Java and ImageJ". In: *BMC bioinformatics* 11.1, pp. 1–7.

Shao, Xinxian et al. (2017). "Growth of bacteria in 3-d colonies". In: *PLoS computational biology* 13.7, e1005679.

Smith, William PJ et al. (2017). "Cell morphology drives spatial patterning in microbial communities". In: *Proceedings of the National Academy of Sciences* 114.3, E280–E286.

Sønderholm, Majken et al. (2017). "Pseudomonas aeruginosa aggregate formation in an alginate bead model system exhibits in vivo-like characteristics". In: *Applied and environmental microbiology* 83.9, e00113–17.

Sousa, Ana Margarida et al. (2013). "Improvements on colony morphology identification towards bacterial profiling". In: *Journal of microbiological methods* 95.3, pp. 327–335.

Stevens, Ann M, Martin Schuster, and Kendra P Rumbaugh (2012). "Working together for the common good: cell-cell communication in bacteria". In: *Journal of bacteriology* 194.9, pp. 2131–2141.

Stoodley, Paul et al. (2002). "Biofilms as complex differentiated communities". In: *Annual Reviews in Microbiology* 56.1, pp. 187–209.

Stubbendieck, Reed M, Carol Vargas-Bautista, and Paul D Straight (2016). "Bacterial communities: interactions to scale". In: *Frontiers in microbiology* 7, p. 1234.

Van Gestel, Jordi et al. (2014). "Density of founder cells affects spatial pattern formation and cooperation in Bacillus subtilis biofilms". In: *The ISME journal* 8.10, pp. 2069–2079.

Vázquez, Alba García (2021a). *ERDA Dataset*. https://sid.erda.dk/sharelink/EZwrOAxEzZ. Accessed: 2021-08-10.

Vázquez, Alba García (2021b). *ERDA Supplementary*. https://sid.erda.dk/sharelink/E55W6FOWOo. Accessed: 2021-08-15.

Wang, Shiwei et al. (2015). "The exopolysaccharide Psl–eDNA interaction enables the formation of a biofilm skeleton in P seudomonas aeruginosa". In: *Environmental microbiology reports* 7.2, pp. 330–340.

Wiki, Image J Documentation (2019). *ImageJ Documentation Wiki*. URL: https://imagejdocu.tudor.lu/gui/process/noise.

Xiong, Liyang et al. (2020). "Flower-like patterns in multi-species bacterial colonies". In: *Elife* 9, e48885.